

## **Thick bottom nepheloid layers in the western Mediterranean generated by deep dense shelf water cascading**

*Pere Puig<sup>a\*</sup>, Xavier Durrieu de Madron<sup>b</sup>, Jordi Salat<sup>a</sup>, Katrin Schroeder<sup>c</sup>, Jacobo Martín<sup>a</sup>, Aristomenis P. Karageorgis<sup>d</sup>, Albert Palanques<sup>a</sup>, François Roullier<sup>e</sup>, Jose Luis Lopez-Jurado<sup>f</sup>, Mikhail Emelianov<sup>a</sup>, Thierry Moutin<sup>g</sup>, Loic Houpert<sup>b</sup>*

<sup>a</sup> Institut de Ciències del Mar (CSIC), Passeig Marítim de la Barceloneta, 37-49. 08003 Barcelona, Spain.

<sup>b</sup> CEFREM, UMR 5110 CNRS-UPVD, 52 Avenue Paul Alduy, 66860 Perpignan Cedex, France.

<sup>c</sup> CNR - National Research Council of Italy, ISMAR - Marine Sciences Institute, Forte Santa Teresa, 19032 Pozzuolo di Lericci, Italy.

<sup>d</sup> Hellenic Centre for Marine Research, 46.7 km Athens-Sounio Avenue, 19013 Anavyssos, Greece.

<sup>e</sup> Laboratoire d'Océanographie de Villefranche (LOV), Université Pierre et Marie Curie, Paris 6, 06230 Villefranche-sur-Mer, France.

<sup>f</sup> Centro Oceanográfico de Baleares, Instituto Español de Oceanografía. Muelle de Poniente s/n. 0715 Palma de Mallorca. Spain.

<sup>g</sup> MIO UM 110 CNRS/IRD/AMU/USTV, , Campus de Luminy, Case 901, 13288 Cedex 09 Marseille, France.

\* Corresponding author. Tel.: 34 93 2309518; E-mail: ppuig@icm.csic.es.

### **Abstract**

The analysis of a compilation of deep CTD casts conducted in the western Mediterranean from 1998 to 2011 has documented the role that dense water formation, and particularly deep dense shelf water cascading off the Gulf of Lions, plays in transporting suspended particulate matter from the coastal regions down to the basin. Deep CTD casts reveal that after the 1999 and 2005-2006 deep cascading events the Western Mediterranean Deep Water (WMDW) was characterized by the presence of a thick bottom nepheloid layer (BNL) that corresponded in thickness with a thermohaline anomaly generated by the mixture of dense waters formed by deep convection in the

open sea and by deep cascading. This BNL can be hundreds of meters thick and in the central part of the basin usually exhibits suspended sediment concentrations of  $<0.1$  mg/l above background levels, reaching higher concentrations close to the continental rise, with near-bottom peaks  $>1$  mg/l. After winter 1999 the BNL spread from the Gulf of Lions and the Catalan margin over the northwestern Mediterranean basin, reaching west of the Balearic Islands and the Ligurian Sea, while after winters 2005-2006 the BNL covered the entire western Mediterranean basin. Thickness and concentration of the BNL tend to diminish with time but this trend is highly dependent on the volume of dense water generated, both by convection and cascading. After winter 1999 the BNL signal vanished in one year, but after winters 2005-2006 it lasted for longer and the turbidity signal can still be distinguished at present (2011). Particle size distribution in the BNL reveals the presence of large aggregates up to 1 mm in size formed by a mixture of single particles with the same bimodal grain size distribution as the surface sediments found in the northwestern Mediterranean slope and basin. Results presented in this paper highlight the fact that the WMDW can be periodically affected by the arrival of new dense waters loaded with suspended particles mainly introduced by resuspension processes during major cascading events, being a key process that could ultimately affect deep-sea biogeochemical cycles in the western Mediterranean.

*Keywords:* bottom nepheloid layer; suspended particulate matter; dense shelf water cascading; open sea convection; sediment transport; Western Mediterranean Transition

## **1. Introduction**

Suspended particles in the oceans play a key role as extractors from, transporters through and sources to the water column of many major and minor elements, being responsible for maintaining most oceanic chemical concentrations (Biscaye and Eittrheim, 1977; Eisma, 1993). Particles are introduced into the ocean by biological production, rivers, glaciers, wind and bottom sediments resuspension. Biological, chemical and gravitational processes then act to remove particles from the water column. These removal mechanism, however, occur on much shorter time scales than the formation, movement or mixing of oceanic water masses, and therefore, particles do not act as pure conservative tracers of water masses, but their presence and

concentration can indicate the location and intensity of oceanographic processes, particularly those involving the resuspension of sediments due to strong bottom currents, and can be used as tracers of water motions (McCave, 1986; Gardner et al., 1990). The redistribution of particulate matter has important implications for understanding and quantitatively modeling biogeochemical processes in the oceans. In the open ocean, surface production is generally the most significant source of particles, but near the continental margins the seafloor can also be an important source of particles as a result of resuspension and lateral advection (Gardner and Walsh, 1990).

The first indirect data on the distribution of oceanic suspended particulate matter (SPM) were obtained in the form of optical parameters or direct filtration measurements (e.g. Ewing and Thorndike 1965, Harris, 1972; Biscaye and Eittreim, 1974; Brewer et al., 1976; Lal, 1977). Data from optical devices suffered the limitation that they were in units of light scattering, attenuation or instrumental parameters such as film density, which were not directly useful to the geologist or geochemist. Subsequently, Biscaye and Eittreim (1977) converted nephelometer data from the Atlantic Ocean water into units of absolute SPM concentrations. In this way, they were able to identify a number of distinctive features in the vertical and horizontal distributions of SPM in the water column. They proposed a conceptual model of the vertical distribution of SPM that can be described as a three-layer model in which the main features are: 1) a surface-water turbid layer, 2) a clear water minimum and 3) a deep-water turbid layer. This three layer model offers a convenient framework to describe the distribution of SPM in the world ocean.

The deep-water turbid layer, also known as bottom nepheloid layer (BNL), was first detected by Kalle (1937) and Jerlov (1953) and it is a remarkable feature of the lower water column in most deep parts of the world ocean (McCave, 1986). The pioneer studies using optical devices revealed that the thickness of the BNL is generally between 500 to 1500 m, and exceptionally can reach up to 2000 m thick. The highest SPM concentrations found in BNLs appear to occur in deep regions (>3000 m depth) affected by strong bottom currents (Eittreim et al., 1976; Kolla et al., 1976; Spinrad and Zaneveld, 1982; McCave 1983). This fact suggests that BNLs are produced by resuspension of the bottom sediments and that their distribution thus indicates the presence of local resuspended particles in the ocean basins. However, their thickness is

generally much greater than the thickness of the bottom mixed layer defined by potential temperature ( $\theta$ ), a fact that precludes the possibility of simple mixing by boundary turbulence being a sufficient mechanism for their formation (Armi, 1978; McCave, 1983). Several studies also pointed out that the broad patterns of the inflow of cold bottom water are very similar to the excess BNL concentration for the southern Indian and Atlantic oceans, suggesting the contribution of particles coming from Antarctic Bottom Water (AABW) in their formation (Kolla et al., 1976, 1978; Eittrreim et al., 1976; Biscaye and Eittrreim, 1977).

One of the regions where the BNL is more developed is the Nova Scotia continental rise, where the High Energy Benthic Boundary Layer Experiment (HEBBLE) was conducted (Hollister and Nowell, 1991). This region is affected by periods of several days to few weeks of high variability of flow speed (over 20 cm/s) and direction reversals associated with increases of water turbidity, defined as abyssal benthic storms (Hollister and McCave, 1984). A careful analysis of these benthic storms revealed that only a small proportion of the peaks in suspended sediment concentration corresponded to local erosion, and that most increased suspended sediment concentration events were clouds of fine suspended material advected into the HEBBLE region (Gross and Williams, 1991). Indeed, BNLs are a complex mixture of particles of local and distant origins, which makes very difficult any attempt to trace their source, even through compositional analysis (McCave, 1986).

In the western Mediterranean basin, the three layer model proposed by Biscaye and Eittrreim (1977) is not generally observed in the numerous deep CTD casts conducted in this area (see MEDAR Group, 2002). The profiles carried out in this epicontinental sea, disregarding the ones conducted over the continental shelf and slope or within submarine canyons, do not show the widely distributed deep BNL that is typically found in large oceanic regions. Nonetheless, data from few CTD surveys contrast with this general finding. The first reference to the presence of a BNL in the western Mediterranean basin is found in Béthoux et al. (2002), who described a 300 m-thick anomalous turbid deep water in the Ligurian Sea during 1999, associated with changes in thermohaline properties of the bottom Western Mediterranean Deep Water (WMDW). These authors attributed the formation of such a BNL to the transport of turbid shelf water and re-suspended sediment by a contemporary major cascading event

of dense shelf water that occurred in the southwestern part of the Gulf of Lions continental margin during winter 1999, although no direct evidence of such a relationship was provided. Later on, Canals et al. (2006) studied the effects of a major cascading event that occurred during winter 2005 and found a well-developed BNL at the mouth of the Cap de Creus submarine canyon that corresponded in thickness with the bottom layer of cold dense shelf water transported to the basin, establishing a causal relationship between the cascading event and the BNL. Since then, no further studies have addressed in detail the characteristics of these ephemeral BNLs, although Puig et al. (2009) explained their formation and spreading as a consequence of the interactions between open sea convection and cascading shelf waters generated during anomalous severely cold winters. This paper aims to expand in this subject, with the goals of characterizing the structure and the spatial and temporal evolution of these observed BNLs in the western Mediterranean basin and better constraining their formation mechanism and relationship with the occurrence of major deep water formation events (i.e. dense shelf water cascading as well as open sea convection).

## **2. Background**

### *2.1. Deep water formation in the northwestern Mediterranean*

Deep water formation is a key process in the thermohaline circulation of the ocean. It occurs over relatively short periods in late winter at just a few locations of the world ocean. It requires a combination of general circulation (gyre driven isopycnal doming) and meteorology (wind driven cooling, evaporation and mixing of surface layer water) to predispose the water column to locally overturn (Marshall and Schott, 1998).

The northwestern Mediterranean Sea is a well-known region where open sea convection and deep water formation can occur on a yearly basis due to winter heat losses and evaporation caused by cold and dry northerly winds. Dedicated experiments in this region started 40 years ago, with the so-called MEDOC Project, and further studies have been carried out since then to advance in the knowledge of such an oceanographic phenomenon. Remarkable sets of publications include the initial MEDOC Group paper (1970), the following comprehensive discussions by Sankey (1973) and Lacombe and Tchernia (1974), the book edited by Chu and Gascard (1991), the reviews published by

Killworth (1983) and Marshal and Schott (1999), and many more. Deep or intermediate convection has been observed several times in the northwestern Mediterranean over the years since 1969, and because of its sensitivity to atmospheric conditions, it is associated with a high interannual variability (Mertens and Schott, 1998).

The water mass distribution in the northwestern Mediterranean comprises four layers. At the surface Atlantic Water (AW), originates from the inflow through the Strait of Gibraltar, and can be distinguished between “recent” and “old” AW according to the residence time in the Mediterranean that increases its salinity. Below it, and mainly during wintertime, cold lenses of Western Intermediate Water (WIW) are found at around 150 m depth. Deeper, a core of warm and salty Levantine Intermediate Water (LIW) –a water mass formed by intermediate (>300 m depth) convection in the eastern Mediterranean that slowly propagates into the western basin through the Sicily Channel– is found, being centered around 400 m depth. Below the LIW layer, the basin is filled with near-homogeneous Western Mediterranean Deep Water (WMDW). The typical potential temperature, salinity and density of these water masses are listed in Table 1 (see also <https://www.ciesm.org/catalog/WaterMassAcronyms.pdf> for further details).

Open sea convection in the northwestern Mediterranean Sea is a three-stage process driven by the atmospheric cooling effect of the strong northern winds. The circulation in this region is cyclonic, which generates a “doming” of the isopycnal surfaces in the center of the cyclonic gyre (Millot, 1987; Font et al., 1988). This results in a weakening of the stratification over a large area, particularly towards late-summer early-autumn, when storm winds and water cooling contribute to mix the surface layer and to progressively erode the seasonal thermocline. This weakening of the vertical stratification is known as the “preconditioning” phase (Stommel, 1972) of the deep convection process.

Later on, during wintertime, intense cold and dry winds begin to blow persistently offshore from the north (Mistral) and northwest (Tramontane), being respectively funneled through the Rhone valley and through the depression between the Pyrenees and the Massif Central. Vertical convection intensifies over a wide area of the northwestern Mediterranean, resulting in a gradual deepening of the surface mixed

layer. The center of the preconditioned area lies directly where the paths of both winds meet and vertical convection in that area can at some point break through the surface stratification down to great depths. A homogenization of the water column in many chimneys of few kilometers horizontal extent occurs within the preconditioning area (Marshall and Schott, 1999). This period is commonly known as the “violent mixing phase”. Accompanying the convection, small scale eddies, usually situated at or near the front dividing overturned and non-overturned water, are formed (Gascard, 1978).

At the end of the period of cold winds, a third phase, the “sinking and spreading phase”, takes place. Observational difficulties have limited the knowledge of what exactly occurs, and recent studies have been undertaken to fully characterize the entire deep convection process. Indeed, the deployment of gliders and of a line moored at 2300 m depth since 2007, and the collection of hydrological profiles enable us to study in detail the evolution of the mixed layer depth in and around the convection area and to examine the exchange processes at the edge of the convection patch (Houpert, 2010). These data also show a rapid restratification by advection of the surface waters during and at the end of the mixing period. With the restratification of the water column, the spreading phase of the newly-formed dense water starts. This dispersion results in particular from the action of anticyclonic submesoscale coherent vortices (radius  $\sim 5$  km and lifetime  $>0.5$  years) that can advect lenses of deep water several hundreds of kilometers away from the formation area (Testor and Gascard, 2003, 2006). Observations collected in the deep basin during the last decade confirm a large interannual variability in the intensity of convection, with the occurrence of unusual deep convection penetrating down to the bottom in 2005, 2006 (Schröder et al., 2008), 2009 and 2010 (Houpert, 2010).

Concurrent with the open sea convection process, dense waters are also formed over the wide Gulf of Lions shelf, which annually cascade downslope until reaching their equilibrium depth (Fig. 1). Although both processes are contemporary and occur in relatively close areas, no specific studies have been conducted to investigate their relationship and the interactions occurring between both types of dense waters.

## *2.2. Dense shelf water cascading off the Gulf of Lions*

Dense shelf water cascading (DSWC) is a climate-driven oceanographic phenomenon occurring not only on high latitude continental margins, but also on mid latitude and tropical margins (Ivanov et al., 2004). DSWC is a specific type of buoyancy driven current, in which dense water formed by cooling, evaporation or freezing in the surface layer over the continental shelf descends down the continental slope to a greater depth. The general DSWC concept was formulated by Fritjof Nansen (Nansen, 1906), who also made the first direct measurements over the Rockall Bank in the North Atlantic Ocean (Nansen, 1913). The term “cascading” was introduced later by Cooper and Vaux (1949), but the same phenomenon is also referred as near-boundary convection (Killworth, 1983) or also as shelf-slope convection, to be differentiated from the open sea convection.

Cascades of DSW can last for several weeks and the associated strong currents can induce erosion and resuspension of surface sediments in the outer shelf/upper slope and generate nepheloid layers (Fohrmann et al., 1998). Such layers can be detached at intermediate levels when the density of the mixture of water and particles reach their equilibrium depth, or if the density is large enough, may evolve into a thick BNL that can reach the lower continental slope and deep basin. This cascading mechanism contrasts with the typical open sea convection, since the latter brings dense surface waters only with particles of biological origin down to the basin.

As it has been stated before, winter heat losses and evaporation induced by persistent, cold and dry northerly winds affecting the northwestern Mediterranean also cause densification and mixing of coastal waters over the Gulf of Lions shelf. Despite the buoyancy gain induced by freshwater inputs, mainly from the Rhone River, once denser than surrounding waters, surface waters over the shelf sink, overflow the shelf edge, and cascade downslope until they reach their equilibrium depth, which changes from year to year depending on the gained density (Millot, 1990; Durrieu de Madron et al., 2005). The first evidences of DSWC in the Gulf of Lions were found in 1953 by Bougis and Ruivo (1954), who identified the formation of dense waters along the southwestern shelf and their cascading into the Lacaze-Duthiers submarine canyon. Further DSWC events in the same area were observed in 1969 by Fieux (1974) and in 1971 by Person (1974), who traced dense shelf waters down to 800 and 350 m depth, respectively. Further evidence was gained during winter 1995 by Lapouyade and Durrieu de Madron



(2001), who observed a cascade at its final stage with a large tongue of cold water escaping the shelf and reaching its neutral density level around 170 m depth. More recently, a fine spatial resolution hydrographic survey performed in 2004 along the axis of the Cap de Creus Canyon (Durrieu de Madron et al., 2005) showed a cold and less salty filament, attached to the seabed, down to 350 m. In all cases, temperature is the main driver of cascading, and the advection of cold and turbid shelf waters produces a turbidity maximum associated with the dense water tongue. At the initial stages of the cascading process, when dense waters escape the shelf and spread around the shelf break depth (150-200 m), they contribute to the formation of the WIW (Dufau-Julliand et al. 2004). In the case that dense shelf waters cascade to deeper levels, they eventually mix with the warmer and saltier LIW layer and with the underlying WMDW.

The monitoring of temperature, current and downward particle fluxes conducted since 1993 in the lower part of the Planier and Lacaze-Duthiers submarine canyons by the *Centre de Formation et de Recherche sur les Environnements Méditerranéens* of Perpignan (CEFREM) revealed an marked interannual variability of the DSWC intensity in the Gulf of Lions (see Heussner et al., 2006 and Canals et al., 2006 for details). Based on these time series, Béthoux et al. (2002) inferred that the 1999 intense DSWC episode, which was traced down to 1000 m depth on the continental slope with down-slope velocities up to 60 cm/s, contributed to the renewal of the bottom waters of the western Mediterranean basin and to the formation of a thin BNL observed in the Ligurian Sea.

Further time series observations in the Gulf of Lions were conducted under the frame of the EuroSTRATAFORM project, during which seven submarine canyon heads were monitored simultaneously in winter 2004. These results revealed that the preferential cyclonic circulation of the coastal current and the narrowing of the shelf at the southwestern end of the Gulf cause most of the water and sediment transport during DSWC events to occur through the Cap de Creus submarine canyon (Palanques et al., 2006). Since then, the occurrence and effects of dense shelf water cascades from the Gulf of Lions have been continuously monitored at the Cap de Creus submarine canyon head, as a complement to the two long-term mooring deployments in the Planier and Lacaze-Duthiers submarine canyons at 1000 m depth. The next major DSWC event recorded by those instrumented moorings took place during the abnormally dry, windy

and cold winter 2005, when cascading was exceptionally intense, lasting for more than three months. This cascading event was well monitored (Canals et al., 2006; Puig et al., 2008) and modeled (Ulses et al., 2008). Under these circumstances, dense shelf waters propagated along and across the continental slope (Font et al., 2007), reaching depths >2000 m where they merged with dense waters formed off-shelf, in the MEDOC area, by the typical open sea convection process. The presence of these two dense waters generated a thermohaline anomaly in the WMDW that spread throughout the entire northwestern Mediterranean basin. The following major DSWC event occurred in winter 2006, which could be also traced down to 1900 m depth by a large network of instrumented moorings deployed in the south-western end of the Gulf of Lions margin under the frame of the HERMES project (Sánchez-Vidal et al., 2008; Pascual et al., 2010; Palanques et al., 2012). The subsequent continuous monitoring at the Cap de Creus and Lacaze-Duthiers submarine canyons, revealed that minor DSWC events occurred in winter 2007 and 2008 (Ribó et al., 2011) and also in winters 2009, 2010 and 2011 (Fig. 2a).

### *2.3. Occasional formation of anomalous deep water masses in the northwestern Mediterranean*

In certain years, besides the typical water masses listed in Table 1, an “occasional bottom water” (BW) is also present in the northwestern Mediterranean. It was detected in 1972-73 and in 1981-82, as a layer deeper than ~2000 m, in which a small positive gradient of both  $\theta$  and S was present down to the bottom (Lacombe et al., 1985; Lacombe 1992). Thus, a layer of minimum  $\theta$  and S appeared at about 2000 m, displaying a V-shape structure in the  $\theta$ -S diagram tail. The differences of  $\theta$  and S between the bottom values and the minimal values at 2000 m were only about 0.01°C and 0.01, respectively. The mechanism of formation and spreading of this BW was unknown, but these preliminary studies concluded that it should not be formed on the shelf and were more likely a result of open sea winter convection near the centre of the cyclonic gyres. The authors pointed out that understanding the process required a careful look throughout the year to the factors affecting  $\theta$ , S and  $\sigma_\theta$  of the surface layer and to the core of the LIW reaching the convection area after having overflowed the Sicilian sill.

The problem of formation of this BW remained open and could be dependent on the properties of the waters making up the LIW, the winter Deep Adriatic Water (EMDW of Adriatic origin) and the Levantine Winter Water (the LIW at its origin). Later on, an effort to investigate the details of the processes involved in the deep water formation both from a theoretical and observational point of view was conducted (e.g. Mertens and Schott, 1998), and a monitoring of LIW flowing through the Sicilian sill was established (see Gasparini et al., 2005).

Béthoux et al. (2002) reported V-shape structures at the end of  $\theta$ -S diagrams in 1999 that they called “ $\theta$ -S anomalies” (see their Figure 3b), corresponding to waters found in the Ligurian Sea below 2000 m, thus having the same properties as the BW previously mentioned. As it has been stated before, this paper also reported the episode of the 1999 deep DSWC in the Lacaze-Duthiers Canyon. The fact that waters affected by the “ $\theta$ -S anomalies” showed an increase of suspended particles corresponding to the previously mentioned BNL lead to the conclusion that such “ $\theta$ -S anomalies” were due to the deep cascading processes. In particular, they discussed about the conditions for deep cascading in terms of atmospheric forcing and performed a review of historical data to find such “ $\theta$ -S anomalies” back to 1972. What they reported were three more episodes, those from CTDs conducted in 1972-73 and 1981-82 corresponding to the BW of Lacombe et al. (1985), and another observed in CTDs conducted in 1988-89. In all cases, at least the first year of each one of the episodes, coincided with periods of strong vertical convection in the MEDOC area (Mertens and Schott, 1998).

Some years later, Lopez-Jurado et al. (2005) reported an abrupt shift in the  $\theta$  and S characteristics of the WMDW observed in March 2005 (see their Figure 3). Subsequently, this shift was highlighted in many papers and scientific documents generated from CTD data obtained in the western Mediterranean since that time (e.g. Salat et al., 2006; Schroeder et al., 2006; Canals et al., 2006; Smith et al., 2008; Schroeder et al., 2008; CIESM, 2009; Schroeder et al., 2010), and also documented through time-series data from the mooring of the CIESM HydroChanges program placed on the lower Catalan slope (Font et al., 2007; CIESM, 2009). Essentially, since 2005, the structure of the WMDW has become more complex with an increase of both  $\theta$  and S from ~800-1200 m downward to a relative maximum, at depths ranging from ~1600 to 2500 m, followed by a decrease of both variables down to the bottom. The

typical signature of this structure in the  $\theta$ -S diagram is a V-shape at the bottom of the classical WMDW signature with a curled end, like a “hook”. This structure suggests the participation of at least two different water types in addition to the ‘classical’ WMDW. The entire signature of this new structure in the  $\theta$ -S diagram apparently was not found in any observation before 2005, but the upper part (i.e., the increase in  $\theta$  and S below the typical WMDW and over the subsequent decrease of both variables) showed the same signature as the above mentioned BW, reported by Lacombe et al. (1985) and the “ $\theta$ -S anomalies” reported by Béthoux et al. (2002). The main difference is that the V-shape ending in the  $\theta$ -S diagram is found more than 1000 m above the previously reported observations, instead of being at the bottom.

Lopez-Jurado et al. (2005) did not identify the two different water sources that generated the anomalous  $\theta$ -S structure, and associated its formation with a strong heat loss during winter 2005, while Schroeder et al. (2006) attributed the anomaly to the effect of the Eastern Mediterranean Transient (EMT) and suggested the contribution of two end members: one water mass with a major contribution of LIW and another with a higher portion of AW. Salat et al. (2006), using CTD data from stations near the Catalan continental slope and from the deep basin, could attribute the sources of this anomalous structure in the  $\theta$ -S diagram to the contribution of newly formed WMDW by open sea convection (i.e. the saltier and warmer water mass) and by cascading (i.e. the fresher and colder water mass). Later, Font et al. (2007) analyzed time series observations from the Cap de Creus Canyon and from the lower Catalan slope during winter 2005 and identified the temporal evolution of the  $\theta$ -S anomaly, which consisted first on the arrival of warmer and saltier waters generated by deep convection, followed by the arrival of colder and fresher waters generated by DSWC.

In the following years, from 2005 onwards, the basic structure of this new WMDW remained unchanged. During winter 2006, the main area of deep water formation was displaced towards the western Ligurian Sea (Smith et al., 2008) and deep cascading off the Gulf of Lions was also reported (see section 2.2.). Schroeder et al. (2008), using data from an extensive CTD survey carried out in late spring 2006, could determine that the thermohaline anomaly filled the entire western Mediterranean basin. The properties of the new WMDW were clearly on the line of the precedent year with slightly higher values of both  $\theta$  and S and maintaining the presence of a hook in the  $\theta$ -S diagrams.

Winters 2007 and 2008 were unusually mild and no signals of deep convection nor cascading were recorded by the moorings located at the lower Catalan slope or in the MEDOC convection area (42°N; 5°E), but the  $\theta$ -S anomaly in the WMDW could still be observed in the Algerian basin (38°N; 5°E) in November 2008 (Schroeder et al., 2010). In winter 2009 and 2010 a new increase in  $\theta$  and S was captured by moored instruments, which was associated with newly produced WMDW (Fuda et al., 2009; Houpert, 2010). In any case, the final situation of the WMDW after winters 2009 and 2010 did not change essentially, since it was still affected by the main changes originated after winter 2005, in what has been recently referred to as the *Western Mediterranean Transition* (WMT) (CIESM, 2009).

### **3. Material and Methods**

#### *3.1. Oceanographic surveys*

Numerous oceanographic cruises have been conducted in the northwestern Mediterranean during the last decades, and the most recent ones were done with CTD probes equipped with fluorescence, turbidity and oxygen sensors. As part of the MEDAR/MEDATLAS II Project, a large compilation of historical oceanographic data was conducted to safeguard and transcode them at a common format and generate an electronic atlas for dissemination of the data among a wide range of users from scientific, educational, industrial, governmental communities (MEDAR Group, 2002). Such a compilation ceased in 2002 and included data from most of the existing, but not all, oceanographic cruises conducted at that time. For the purpose of this paper, a focused survey was conducted to have access to as many as possible deep CTD casts performed in the western Mediterranean during the last decade to illustrate the distribution of hydrographic properties and nepheloid layers in this region and characterize their evolution, especially before during and after intense surface water convection and cascading events. Since the last deep cascading events occurred in 1999 and in 2005-2006 (Fig. 2), our compilation started in 1998 and ended in 2011. This selection mainly includes deep CTD stations in the North Balearic Basin with casts profiling the entire water column (with the exception of two cruises that have profiles just down to 2000 m depth). The selected cruises are listed in Table 2, along with the

turbidity sensor used during each survey. Additionally, in winter 2011, during the CASCADE cruise, an Underwater Vision Profiler was added to the CTD probe, which allowed quantification of the number of particles between 60  $\mu\text{m}$  and 26 mm and of large zooplankton (Gorsky et al., 2000). In addition, large volumes of water were filtered during the same cruise to characterize the nature of the particles within the BNL. Regarding the new salinity scale TEOS-10 (IOC, SCOR and IAPSO, 2010) we have used the Practical Salinity ( $S_p$ ) PSS-78.

### *3.2. Turbidity sensors*

The turbidity sensors used in these cruises were either transmissometers (Sea Tech Inc. and WET Labs C-Star) or optical backscatter sensors (Seapoint).

Transmissometers use a Light Emitting Diode (LED) with a wavelength of 660 nm and a beam diameter of 15 mm. The receiving sensor is located at some fixed distance (pathlength) from the emitting diode and the return signal is inversely proportional to the concentration of suspended particles in the water (Baker and Lavelle, 1984; Bishop, 1986). Either 25, 20 and 10 cm path-length transmissometers were used depending on the cruise (Table 2).

Seapoint optical backscatter sensors measure turbidity by detecting the scattered light from suspended particles present in a small volume of water within 5 cm of the sensor windows. The light sources are 880 nm LEDs and the light detectors are silicon photodiodes with visible light blocking filters. The amount of scattered light that reaches the detector is proportional to the turbidity or particle concentration in the water over a very large range.

### *3.3. Turbidity signal calibration*

The turbidity signal recorded by transmissometers is generally reported as beam attenuation coefficient (BAC). The transmissometer measures a voltage ( $V$ ) proportional to the transmitted light intensity at a distance ( $L$ ) from the light source:

$$V = V_0 e^{-CL}$$

where  $V_0$  is the voltage in air,  $L$  is the beam pathlength and  $C$  is the total BAC. Since  $C$  has contributions from pure water ( $C_w$ ), suspended matter ( $C_p$ ) and dissolved organic matter ( $C_y$ ), and it is known that  $C_y = 0$  at the red part (660 nm) of the light spectrum (Jerlov, 1968), then

$$C_p = (-1/L) \ln (V/V_0) - C_w$$

Generally  $C_w$  values are around  $0.36 \text{ m}^{-1}$  (e.g. Bishop, 1986; Hall et al., 2000). However, for practical purposes,  $C_w$  is usually considered as the minimum BAC measured during an oceanographic cruise/transect and the calculated  $C_p$  reflects the variations over this background level, despite the fact that several studies have shown that the SPM concentrations in the clear water minimum can be quite variable (e.g. Eitrem and Ewing 1974; Brewer et al., 1976).

The turbidity signal measured by optical backscatter sensors is factory adjusted for a consistent response to a Formazin Turbidity Standard, and the reported values are expressed in Formazin Turbidity Units (FTU).

Both  $C_p$  and FTU values can be converted into suspended sediment concentration (SSC) using simple regression equations. Since  $C_p$  only reflects the contribution from particles above the clear water minimum, the reported concentrations should be considered as excess SSC (xs-SSC). Consequently, for easy comparisons between both types of sensors, the lowest FTU measured during an oceanographic cruise/transect in the clear water minimum has been also attributed to the background concentration of suspended particulate matter. For the purpose of this paper, the general equations described in Guillén et al. (2000) for the western Mediterranean, in particular  $C_p$  for the Ebro margin and FTU for the North Balearic Sea, have been used to convert the different type of turbidity units into xs-SSC, expressed in mg/l. These equations are:

$$\text{xs-SSC} = 1.48 C_p$$

$$\text{xs-SSC} = 0.79 \text{ FTU}$$

In some of the studied cruises, the CTD probe was equipped with both type of turbidity sensors and this fact allowed us to verify the correct use of this general equations. Overall, both sensors reproduce quite similarly the nepheloid structure, regardless of their different optical principles (transmission vs. backscatter), and the used equations seem to provide comparable  $x_s$ -SSC values throughout the entire water column (Fig. 3). Similar results comparing different type of sensors have been obtained elsewhere (e.g. Hall et al., 2000, their Figure 5), despite the fact that backscatter is more affected by fine particles and transmission by coarse particles, and that many factors (i.e. particle size, shape, composition, and aggregation/flocculation) influence optical measurements (Downing, 2006; Boss et al., 2009; Hill et al., 2011).

#### *3.4. Suspended particles size spectra*

The Underwater Vision Profiler (UVP, generation 5) is an optical instrument coupled to the CTD-Rosette package (Picheral et al., 2010). It acquires focus images in a virtual volume of water delimited by a light sheet issued from red light-emitting diodes (LEDs) of 625 nm wavelength at a frequency up to 6 Hz. The smaller size limit is fixed by optical resolution, whereas the larger size limit is determined by the volume of water illuminated per image. Recorded images are automatically digitized, classified and analyzed, and the results are expressed as abundance and/or size distributions. It enables to quantify the vertical distribution of macroscopic particles and zooplankton between 60  $\mu\text{m}$  and 26 mm in size.

In parallel to in situ measurements, large water volumes (12 L) were collected in the BNL near the seabed in March 2011. Water samples were filtered up to filter saturation on pre-weighed Nuclepore filters of 0.4  $\mu\text{m}$  pore size. Dry filters were later sonicated in pure water in the laboratory, and the disaggregated suspended matter collected was analyzed in a laser particle sizer to provide the size distribution of primary particles.

## **4. Results**

As it has been stated in the introduction section, one of the goals of this paper is to characterize the vertical structure, as well as the spatial and temporal evolution of BNLs



in the western Mediterranean basin after the last deep DSWC events (i.e. winters 1999 and 2005-2006).

Figure 4 shows the location maps at two different scales of the compiled CTD casts with a color code for each year considered in this study. Given the large number of CTD casts compiled and their variable spatial distribution, the results presented in this section have been ordered chronologically providing a snapshot (i.e. a single profile) of the prevailing deep hydrographic and nephelometric structures representative of each year. When data distribution permitted it, hydrographic sections have been also presented. Figure 4b also indicates the location of the specific casts or sections illustrated in the following figures, to help the reader to situate them geographically.

#### *4.1. SSC of clear water minimum*

Whereas  $x_s$ -SSC values will be presented and discussed hereafter, it is noteworthy to mention here what are the absolute concentrations we are effectively dealing with. A conversion of the optical signal into SSC has been given to estimate the  $x_s$ -SSC above a background concentration corresponding to the clear water minimum. This minimum was generally found in the middle of the water column, between 1000 and 2000 m depth. Gravimetric measures of SSC obtained in the clear water minimum are scarce, but recent data collected during the CASCADE cruise (Table 2) indicate concentrations between 0.05 and 0.08 mg/l for the northwestern Mediterranean. Such background concentrations should be added to the  $x_s$ -SSC values shown in the following Figures.

#### *4.2. The 1999 cascading event*

Figure 5 displays classical potential temperature, salinity and turbidity profiles in the northwestern Mediterranean showing the four water masses found in this region (Table 1). This cast was collected at the Gulf of Lions continental rise on 4 April 1998 during the FETCH-98 cruise. The signatures of AW, WIW, LIW and WMDW could be clearly distinguished in the potential temperature and salinity profiles and the  $x_s$ -SSC showed a well-developed surface nepheloid layer (SNL) spanning from the surface down to 800 m depth. Deeper in the water column, the  $x_s$ -SSC maintained constant values close to zero down 2128 m depth, few meters above the bottom, without showing any increment

that could be associated with a BNL. The same water mass structure and the lack of BNL was observed on 23 July 1993 during the DISCOVERY-93 cruise (data not shown), indicating that in the absence of deep cascading between both cruises (Fig. 2), the WMDW characteristics remained quite stable.

On 21 February 1999, during the HIVERN-99 cruise, a deep CTD cast was conducted on the northern Catalan margin westward from the MEDOC area (Fig. 6). This cast nicely captured the deep convection process occurring in that year during wintertime showing almost constant values of  $\theta$  (12.89-12.91° C) and  $S_p$  (38.44-38.47) from the sub-surface down to 1600 m depth. The xs-SSC profile showed a thin SNL associated with slightly warmer and fresher waters at the surface; while a constant clear water minimum (CWM) was associated with the convection waters. Deeper in the water column, at 1620 m water depth, colder, fresher and more turbid water was found down to the bottom. The origin of these waters differs from the deep convection process as their  $\theta$  and  $S$  values reflect the arrival of the 1999 deep DSWC event down to the basin. This dense shelf water generated a ~600 m-thick BNL, reaching mean xs-SSC of ~0.08 mg/l and isolated maximum values up to 0.2 mg/l in the water parcel that showed the coldest (12.84° C) and freshest (38.46) values.

Four days later, on 25 February 1999 and during the same HIVERN-99 cruise, another deep CTD cast was conducted in the Valencia Valley, half-way between the Catalan coast and the Balearic Islands (Fig. 7). In this location, the  $\theta$  and  $S_p$  profiles did not show evidence of convection, since AW, WIW, LIW and WMDW were clearly present. However, between 1750 m and the bottom, a positive thermohaline anomaly was found and was characterized by having high xs-SSC up to 0.1 mg/l, developing a ~600-m-thick BNL.

One year later, on 6 February 2000 and during the HIVERN-00 cruise, another deep CTD stations was conducted in the Valencia Valley (Fig. 8). This cast also showed the typical presence of AW, WIW, LIW and WMDW, but below 1800 m depth a weak but noticeable positive thermohaline anomaly was still observed. The anomaly at this station was only ~200-m thick and was still associated with a weak BNL characterized by a slight increase of xs-SCC of 0.02 mg/l. Other deep CTD casts from this cruise (not shown) also reflected the presence of the positive thermohaline anomaly, but not all of

them had the associated increase of xs-SSC close to the bottom, therefore the BNL observed in 1999 faded away approximately after one year.

#### *4.3. The 2005-2006 cascading events*

On September 2004, during the EFLUBIO-1 cruise, a couple of deep CTD casts were conducted in the northwestern Mediterranean basin. Although those profiles did not reach deeper than 2000 m due to a depth rate limitation of one of the CTD sensors, the water masses and the distribution of xs-SSC before the 2005 deep cascading event could be well established. In the cast conducted on 18 September 2004 in the MEDOC zone at 42°N; 3°E (Fig. 9), the seasonal WIW was missing and the surface AW was associated with a weak SNL. Below it, the LIW and the WMDW were particle-free and the xs-SSC profile showed values close to zero from 200 down to 2000 m water depth.

On 24 March 2005, during the EFLUBIO-2 cruise, a hydrographic section on the Catalan margin off Barcelona captured the formation of the BNL associated with the cascading of dense shelf waters that occurred in winter 2005 (Fig. 10). The shallower profile revealed the presence of a turbid and dense water mass filling almost the whole water column (from 50 to 300 m water depth) with a homogeneous and extremely dense water for such shallow depths ( $\sigma_\theta > 29.14 \text{ kg/m}^3$ ) occupying the lowermost 100 m and reaching xs-SSC of  $\sim 0.3 \text{ mg/l}$  near the bottom. The same dense water mass could be observed in the next CTD profile, at 720 m depth, generating a sharp density gradient at 420 m water depth and filling the lowermost water column down to the bottom. This 300-m thick dense water mass was associated with a BNL that increased its xs-SSC with depth, from  $0.1 \text{ mg/l}$  just below the density gradient to  $0.4 \text{ mg/l}$  above the seafloor. Deeper in the margin, on a CTD profile conducted at 1350 m depth, the density gradient was less evident. However, a noticeable change in density associated with the development of the BNL occurred at 700 m water depth. The BNL became thicker and reached and maintained xs-SSC  $\sim 0.4 \text{ mg/l}$  in the lower 300 m of the water column. A similar situation was found in the next CTD profile conducted at 1680 m depth, and the slight change in density was observed at 770 m water depth. The BNL became even thicker (900 m) and increased the xs-SSC with depth until reaching  $0.5 \text{ mg/l}$  around 30 meters above the seafloor.

During the same cruise, the CTD station conducted in the MEDOC zone in the preceding year (Fig. 9) was revisited on 29 March 2005, and the water structure and particle distribution down to 2000 m water changed dramatically due to the winter 2005 deep convection and cascading events (Fig. 11). The most remarkable feature was the presence of a thick positive thermohaline anomaly spanning from 750 m water depth down to the bottom associated with a well-developed BNL. Such a thick (i.e. 1500 m) BNL increased progressively its concentration with depth and reached xs-SSC of 0.1 mg/l at 400 meters above the seafloor, where the CTD stopped.

The arrival to the basin of dense shelf waters generated during the winter 2005 deep cascading event was nicely captured by a deep CTD cast conducted on 26 April 2005 at the mouth of the Cap de Creus Canyon, 2145 m depth, during the STRATA-3 cruise (Fig. 12). The thermohaline anomaly and the progressive increase of turbidity started at 560 m water depth, and below 1840 m water depth, much colder, fresher and turbid waters were found. The lowering in temperature and salinity and the increasing in turbidity occurred in a stepwise manner, with sharp gradients at 2050 and 2130 m water depth. The lowermost water mass reached xs-SSC  $\sim$ 1.2 mg/l and exhibited high values of chl. *a* fluorescence (not shown) indicative of the near-bottom intrusion of chlorophyll-rich and turbid dense shelf water (see Canals et al. (2006), their Figure 3).

One year later, on 23 April 2006 and during the HERMES-3 cruise, a deep CTD cast was also conducted in the MEDOC zone, immediately after another deep convection and cascading event (Fig. 13). This cast revealed a similar water structure and particle distribution compared to the one from the preceding year. The beginning of the positive thermohaline anomaly was located at 590 m water depth, while the beginning of the BNL was found at 1130 m water depth, approximately where the anomaly reached its maximum values in  $\theta$  and  $S_p$ . From that depth down to the bottom,  $\theta$  and  $S_p$  decreased slightly and the xs-SSC progressively increased. The BNL became more concentrated below 2070 m water depth, associated with a colder and fresher water mass that occupied the lowermost part of the water column, reaching xs-SSC  $\sim$ 0.1 mg/l in the last 40 m above the seafloor.

#### *4.3. The 2007-2011 period*

The MEDOC region was revisited one year later during the HERMES-6 cruise on 3 July 2007. The deep CTD cast conducted at that time evidenced the persistence of the positive thermohaline anomaly and the maintenance of the associated BNL (Fig. 14). In this profile, the thermohaline anomaly started at 1160 m water depth and reached its relative maximum in  $\theta$  and  $S_p$  at  $\sim 1580$  m water depth, which was approximately the depth where the BNL started to develop. Deeper in the water column,  $\theta$  and  $S_p$  progressively decreased towards the bottom, while the xs-SSC increased until reaching maximum values  $\sim 0.07$  mg/l very close to the seafloor.

In 2008 and during the DEEP-1 cruise, two CTD casts were collected on 29 March at the time that deep convection was taken place. The signature of the LIW core was degraded and a homogeneous profile of  $\theta$  and  $S_p$  could be observed down to 980 m water depth (Fig. 15), indicating the limit of open sea deep water convection. These shallow waters showed relatively high values of xs-SSC ( $\sim 0.08$  mg/l) through the water column until reaching the clear water minimum just below the maximum depth of convection. The positive thermohaline anomaly begun at 1460 m water depth, while the relative maximum in potential temperature and salinity and the development of the BNL started at 1890 m water depth. Close to the bottom, in the lower 100 m of the profile, the BNL increased its xs-SSC from  $\sim 0.02$  to  $>0.12$  mg/l, reaching near-bottom concentrations higher than in the preceding years.

As it has been mentioned in section 2.1, in winters 2009 and 2010 the open sea deep convection affected the entire water column. After the convection period, during the FAMOSO-2 cruise in April-May 2009, the water column was re-stratified but the positive thermohaline anomaly and the associated BNL was still noticeable on 3 May (Fig. 16). The anomaly was uplifted and started at  $\sim 710$  m water depth and the typical relative maximum in  $\theta$  and  $S_p$  (at the same depth) was less evident. The BNL did not show any sharp increment and progressively increased its concentration towards the bottom, where it reached xs-SSC of  $\sim 0.08$  mg/l.

In September 2010, the MEDOC zone was revisited during the DEEP-5 cruise and the CTD casts still revealed the presence of the thermohaline anomaly and the development of the BNL (Fig. 17). The beginning of the anomaly was located at 1120 m water depth and towards the bottom showed small fluctuations in  $\theta$  and  $S_p$ . In this profile, conducted

on 16 September, the BNL was thinner and less concentrated than in the spring of the preceding year, and it began to develop at ~200 m above the seafloor, reaching maximum values of xs-SSC ~0.04 mg/l.

In winter 2011, during the CASCADE cruise, the open sea convection zone was intensively sampled to study the deep convection process and numerous deep CTD casts distributed along two hydrographic sections were conducted from 1-22 March 2011 (Fig. 4), at the time and immediately after the convection phase had taken place. Hydrographic data collected during the cruise suggested that in winter 2011 open sea convection also reached the seafloor. An example of the hydrographic and nephelometric structure observed during the cruise on 6 March is presented in Figure 18. At that station, a quasi-homogeneous  $\theta$  and  $S_p$  profile associated with the open sea convection process was observed from ~100 m down to ~1700 m water depth. Such homogeneous water mass had low xs-SSC values, although it showed a progressive increase in turbidity with depth with some relative maxima at intermediate levels. Below 1900 m water depth, a colder, fresher and more turbid water mass was found, which formed a 270 m thick BNL. At 2050 m depth, coincident with a subtle increase of  $\theta$  and  $S_p$ , a relative clear water minimum was seen and below it the xs-SSC sharply increased to values ~0.6 mg/l.

The station in the middle of the convection region (i.e. where the two hydrographic sections crossed, Figure 4) was reoccupied several times during the CASCADE cruise to assess the short-term variability of the BNL. Whereas the depth of the clear water minimum did not vary significantly, the water column between 500 and 1000 m depth became very clear with intrusion of the LIW during the restratification phase (not shown). The BNL was always present but showed a large variability among profiles collected at the same station in few hours to several day time intervals, both in thickness and concentration, with differences up to one order of magnitude (from 0.04 to 0.72 mg/l) in the near-bottom xs-SSC (Fig. 19). Variations of turbidity were associated with slight fluctuations of  $\theta$  ( $\Delta\theta=0.01^\circ\text{C}$ ) and  $S_p$  ( $\Delta S_p=0.004$ ).

#### *4.5. Nature and size distribution of particles in the BNL*

Data collected in March 2011 during the CASCADE cruise also allowed characterizing the type of particles in the BNL and their relative size (Fig. 20). The profile shown in this figure displays similar turbidity (FTU) and even higher BAC in the convection waters (characterized by high fluorescence values), but, in the BNL, an increased amount of large (i.e. 60  $\mu\text{m}$  - 26 mm) particles can be clearly identified using the UVP measurements. The number of large particles increases with depth, but their particle size distribution is fairly homogeneous throughout the entire BNL. Depth-averaged particle size distribution showed a relative minimum around 100  $\mu\text{m}$  and a peak around 150  $\mu\text{m}$  and progressive decreases of the volumetric concentration of larger particles until reaching a maximum of 1 mm in size (Fig. 21a). Images of large particles in the BNL (not shown) indicate that they are amorphous aggregates and that there is an almost nil contribution of planktonic organisms. Depth-averaged particle size distribution completed in the laboratory for disaggregated (i.e. sonicated) suspended particle samples collected on filters gave access to the primary particles size distribution. The analysis showed that primary particles spectra is bi-modal and is mainly composed of very fine particles of less than 2  $\mu\text{m}$  and fine particles between 4 and 50  $\mu\text{m}$  (Fig. 21b). This distribution is typical of silty and clayey deep sediments of this region (Fig. 21c).

## **5. Discussion**

### *5.1. Formation of the BNL and relationship with the thermohaline anomaly*

Data presented in this paper indicate a clear relationship between the thermohaline anomaly generated after major deep cascading and convection events and the formation of a thick BNL in the northwestern Mediterranean. This thermohaline anomaly corresponds in part to the water mass previously known as “occasional bottom water” (BW), identified by Lacombe et al. (1985), whose origin was not clearly discerned (see section 2.3).

The best cruise to illustrate the formation of the thermohaline anomaly and associated BNL is the HIVERN-99, since one profile conducted in the northern Catalan margin captured the convection process from the surface down to 1620 m water depth and the

near-bottom intrusion of colder, fresher and turbid water generated by cascading off the Gulf of Lions (Fig. 6). The profile conducted few days later in the Valencia Valley just showed a positive thermohaline anomaly generated by the mixture of the two dense water masses and the presence of the BNL (Fig. 7). The combination of the two profiles in a  $\theta$ - $S_p$  diagram reproduces nicely a “hook” shape in the lower part of the profiles, which allows us to identify the two end members (i.e. convection and cascading) that generated the anomaly (Fig. 22). The convection end member corresponds to the relative maximum of  $\theta$  and  $S_p$  from the “hook” and the cascading end member to the relative minimum of  $\theta$  and  $S_p$  towards the end of the profile. As it has been mentioned in section 2.3, Béthoux et al. (2002) identified in two deep CTD casts from the Ligurian Sea collected in June 1999 positive  $\theta$ - $S_p$  and turbidity anomalies, which were associated with the 1999 deep cascading event. However, these profiles showed only the rising part of the anomaly (see their Figure 3b), and therefore the anomalies corresponded more precisely to the mixture of the convection and cascading waters that spread throughout the basin and reached the Ligurian Sea few months later.

The thermohaline anomaly in the WMDW after winter 2005 had the same origin and both dense waters generated by convection and by cascading contributed to its formation, as was initially pointed out by Salat et al. (2006) and Font et al. (2007). It has to be taken into account that the suspended particles that generate the BNL come mainly from the cascading waters (see Figs. 6 and 10), since open sea convection waters may only carry biogenic particles from the surface to the bottom.

The formation of the anomalies in  $\theta$  and  $S_p$  in the northwestern Mediterranean after winters 1999 and 2005 and their relationship with the BNL can be summarized in an historical series of  $\theta$ - $S_p$  diagrams with the  $x_s$ -SSC parameter represented in color code (Fig. 23). In 1998, the lower part of the  $\theta$ - $S_p$  diagram showed a continuous decrease of  $\theta$  and  $S_p$  with depth, at a nearly constant  $\sigma_\theta$  of  $29.10 \text{ kg/m}^3$ , while in 1999, the thermohaline anomaly was well developed, showing higher  $x_s$ -SSC near the bottom, particularly in the decreasing part of the “hook”. One year later, the thermohaline anomaly only showed the rising part of the “hook” and the  $x_s$ -SSC values were extremely low, suggesting the disappearance of the BNL after year 2000. The lack of deep cascading (Fig. 2) and deep convection (Herrmann et al., 2010) from year 2000 to 2004 resulted in a period with a typical WMDW occupying the basin. However, in 2005



the anomaly and BNL was reproduced again after the mixing of deep convection and cascading waters, but instead of vanishing in few years, it has been maintained until present (year 2011), with small variations caused by the deep convection events from winter 2009 and 2010 (Houpert, 2010).

### *5.2. Lifetime of the BNL*

The temporal evolution of the BNL and associated thermohaline anomaly after winter 1999 and 2005 differs considerably. The 1999 BNL and anomalous WMDW vanished after one year, showing a behavior similar to the previous observations of “occasional bottom waters”, whereas the 2005 ones have become a permanent feature in the western Mediterranean basin until present (2011), as a major signature of the WMT (CIESM, 2009). The explanation for such a difference seems to be related with the volume of dense waters generated in each year, and therefore, in the initial thickness of the thermohaline anomaly and associated BNL.

Dufau-Julliand et al. (2004) computed numerically the volume of dense waters (attributed to WIW) generated by cascading during winter 1999 and estimated an amount of  $500 \pm 125 \text{ km}^3$  reaching depths greater than 400 m. Their model could not exactly reproduce the temperature observations at 1000 m depth within the Lacaze-Duthiers submarine canyon (Fig. 2) and the authors pointed out that the total volume could be underestimated. To our knowledge, there are no quantifications of the volume of dense waters generated by convection during winter 1999. The volume of dense shelf waters generated during winter 2005 was estimated by Ulses et al. (2008) and accounted for a total of  $2,350 \text{ km}^3$ , four times the estimates of the 1999 DSWC event and corresponding to an annual average formation rate of  $\sim 0.07 \text{ Sv}$ . The open sea convection during the same winter was also modeled by Herrmann et al. (2010) and the estimated volume reached  $36,600 \text{ km}^3$ , corresponding to a yearly formation rate of  $1.16 \text{ Sv}$ . Although the volume of dense waters (i.e. convection and cascading) during winter 2006 has not been computed yet, Schroeder et al. (2008) estimated from CTD observations that the cumulative formation of anomalous dense water for winters 2005 and 2006 was approximately equal to  $2.4 \text{ Sv}$ , and revealed that in less than two years almost the whole western Mediterranean basin was filled with this new deep water, renewing and uplifting the formerly resident WMDW.

The difference in the volume of deep water generated on each winter presumably controlled the initial thickness of the BNL and of the thermohaline anomaly, being in the northwestern Mediterranean approximately 650 m and 1500 m-thick after winter 1999 and 2005, respectively (Figs. 5, 6 and 10). Their thickness decreased away from the dense water formation region and their spatial extension also differed between years. In June 1999, after the 1999 cascading event, the BNL reached the eastern side of the Balearic Islands and the Ligurian Sea, while in April-May 2005, after the 2005 cascading event, it covered most of the northwestern Mediterranean basin (Fig. 24). In June 2006, after the contribution of the deep cascading and convection in winter 2006, the BNL covered the entire western Mediterranean basin (Fig. 24). These maps do not differ from the ones generated by Béthoux et al. (2002) for the 1999 thermohaline anomaly and Schroeder et al (2008) for the 2005-2006 thermohaline anomaly, but it is worth to highlight that the suspended particles within the BNL, which originated mainly in the Gulf of Lions and Catalan margins, travelled large distances along with the anomalous dense waters. In fact, deep CTD casts conducted in July 2008 during the trans-Mediterranean cruise BOUM (Moutin et al., 2011) still evidenced the presence of a BNL in the entire basin.

While the observations conducted immediately after winter 2005 showed a thick BNL that matched the thermohaline anomaly in thickness, observations in the following years demonstrated that the BNL became thinner and restricted to the lowermost water mass characterized by colder and fresher values (i.e. the decreasing part of the “hook”; Fig. 23). This suggests that there is a progressive removal of particles from the water column and concentration of them in a near-bottom turbid layer, possibly helped by the dilution effect of the upper part of the BNL by newly formed clear dense water by open sea-convection in winter 2007 and 2008, which did not reach the bottom.

The increased thickness and higher concentration of the BNL observed after winter 2009 (Fig. 16) was not related to new resuspended particle inputs from DSWC, since in that year cascading was mild (Fig. 2). Such increases were presumably created by local resuspension processes associated with the bottom-reaching open sea convection in winter 2009, which occupied most of the deep basin off the Gulf of Lions (Houpert, 2010, Stabholz et al, 2012). Deep sea currents measured in the northwestern

Mediterranean basin during normal conditions (i.e. without dense water formation) show average velocities of ~3-4 cm/s and sporadic maximum values ranging between 12 and 21 cm/s (Millot, 1985; Puig et al., 2001; Font et al., 2007; Palanques et al., 2009; Houpert, 2010). These weak current velocities would favor particle settling in an almost quiescent environment. However, during bottom reaching open sea convection events, deep currents in the northwestern Mediterranean basin can increase to sustained values >35 cm/s (Palanques et al., 2009; Martín et al., 2010; Salat et al., 2010; Stabholz et al., 2012). The capacity of these high currents to induce active sediment resuspension was documented by Martín et al. (2010) and Stabholz et al. (2012) by means of data from current meters and sediment traps data deployed at several depths in the Ligurian Sea and the Gulf of Lion respectively. Currents during the deep convection event that affected these regions in winters 2006 and 2009 were strong (20-40 cm/s) and similar in the whole water column, while particle fluxes collected by sediment traps increased near the bottom by two orders of magnitude. The same resuspension process was also observed by moored instruments at the mouth and southern slope of the Cap de Creus submarine canyon in winter 2006, where near-bottom turbidity peaks (up to 6 mg/l) occurred during current increases (~30 cm/s) induced by deep open sea convection (Palanques et al., 2011). In winter 2010, open sea convection in the northwestern Mediterranean reached again the basin seafloor (Houpert, 2010), as well during winter 2011 (this paper) and the associated strong currents likely contributed to resuspend the recently deposited particles.

During the CASCADE cruise in March 2011, the same CTD station was revisited on several occasions and the thickness and concentration of the BNL varied greatly with time (Fig. 19). The same variability was observed in nearby CTD casts along the same transect at stations conducted consecutively, suggesting that the BNL was not homogeneous and that there were parcels of highly turbid water (xs-SSC ~0.7 mg/l) surrounded by regions of clearer water but still showing a weak BNL (xs-SSC ~0.04 mg/l). The fact that the highly concentrated BNL was located in a relatively small and isolated region could indicate that deep convection reached more intensively that area, causing a local resuspension that would move with currents and spread along the basin refueling the BNL. What remains unclear from the analyzed dataset is if the deep open sea convection process alone can create enough bottom sediment resuspension to generate such thick BNLs, without the occurrence of a concurrent (or recent) deep

DSWC event that previously supplied large amounts of unconsolidated particles to the basin seafloor.

### *5.3. Suspended particles in the BNL*

Most of the particles resuspended during the 2005 cascading event settled to the seafloor quite rapidly (i.e. during March 2005), as it could be observed in the downward particle fluxes collected by a sediment trap deployed in the Gulf of Lions continental rise (see Palanques et al., 2009, their Figure 6). Gonzalez and Hill (1998) stated that in sediment suspensions, after an initial period of particle flocculation and rapid settling, the concentration of the remaining particles is such that the time scale for further aggregation becomes large, effectively stranding this remaining particle population in suspension. In coastal environments, as in the case of the Po River and Adriatic Sea, this stranded population is made up of small, single grains and microflocs that can be transported at long distances (Mikkelsen et al., 2006; Milligan et al., 2007). Therefore, the particles forming the BNL in the northwestern Mediterranean would presumably correspond to a stranded population which could last as long as the water mass in which they are confined will be present in the basin.

Images collected by the UVP during the CASCADE cruise revealed that the BNL found in the western Mediterranean is composed by large particle aggregates of mainly 150  $\mu\text{m}$  in size and that the larger flocs can reach 1 mm (Fig. 21). Asper (1986) and Gardner and Walsh (1990) found deep-water maxima of large porous aggregates in the Panama basin and in the northern Gulf of Mexico continental slope, respectively, which were ascribed to resuspension and advection from margin boundaries. Asper (1986) proposed that this flocculated material could be transported at large distances from its origin, and remain essentially in suspension until it is scavenged by fast-sinking material and removed from the water column. Calculated settling speeds indicated that, on average, larger aggregates (4-5 mm) settled more slowly ( $1 \text{ m day}^{-1}$ ) than smaller aggregates (1-2.5 mm,  $36 \text{ m day}^{-1}$ ), suggesting that larger aggregates are less dense (i.e. more porous) than smaller aggregates (Asper, 1987). The large surface areas of these flocculated particles make them optically significant, even at very low mass concentration (Mikkelsen et al., 2006), and therefore can create a noticeable signal to the turbidity sensors usually mounted on CTDs (both transmissometers and optical backscatter

sensors, see Figure 20 as an example). The aggregates in the western Mediterranean BNL are smaller than the ones reported in the literature, but they have probably low densities and slow settling velocities as well. The turbulent motions and the negligible water density gradient in the deep layer thus may enable the persistence of particles in suspension for years.

In situ and laboratory size distribution of sonicated suspended particles in the BNL show the predominance of clays, the presence of fine silts and the absence of coarser particles in these aggregates. The agreement between sonicated particle size distributions of suspended particulate matter within the BNL and the bottom sediments (Fig. 21) indicate that individual particles are mainly composed by resuspended superficial sediment from slope and basin regions, in agreement with the BNL origin linked to major DSWC events off the Gulf of Lions.

The transport of resuspended material from the continental margin to the basin and the formation of these BNLs, both after winter 1999 and winter 2005, are considered to be responsible for the fertilization of the western Mediterranean deep-sea environment. This could be demonstrated by the enhanced recruitment of deep-sea biological populations after deep cascading events (Company et al., 2008), which was attributed to the arrival and spreading of nutritive particles (from the shelf and upper slope) to the basin seafloor. The formation of such BNLs after deep cascading events highlights the fact that the WMDW can be periodically modified by the arrival of resuspended particles, being a key process that could affect significantly the biogeochemical cycles in the western Mediterranean.

## **Conclusions**

The characteristics of thermohaline and turbidity structures observed in the deep basin of the western Mediterranean during 1998-2011 allow us to draw the following conclusions:

- A thick BNL is intermittently formed in the northwestern Mediterranean basin after deep DSWC events off the Gulf of Lions and Catalan margin.

- The observed BNLs equate in thickness with the thermohaline anomalies generated by the mixture of dense waters formed by deep cascading and deep convection at the open sea. Such thermohaline anomaly corresponds to the water mass previously known as “occasional bottom water”, whose origin was not clearly identified.
- Thickness, spreading and persistence of the BNL seem to be related to the volume of deep dense waters formed, both by cascading and open sea convection. The BNL generated after the 1999 cascading event lasted approximately one year and affected the northern sub-basin, while the BNL generated after the 2005 cascading event covered the entire basin and can be still observed at present (2011). The following winter of 2006 with deep dense water formation, both by cascading and convection, and the further deep convection winters (without deep cascading) in 2009, 2010 and 2011 have contributed to the BNL maintenance.
- The present BNL includes a stranded particle population partially composed by large aggregates mostly of 150  $\mu\text{m}$  and up to 1 mm in size with apparent low densities and slow settling velocities.
- The quasi-permanent presence of a BNL in the western Mediterranean is a consequence and feature of the Western Mediterranean Transition (WMT) that, besides increasing the amount of suspended particles in the WMDW, could have the potential to modify the deep-sea biogeochemical cycles of this semi-enclosed basin.

### **Acknowledgements**

This research was supported by EU projects EuroSTRATAFORM (EVK3-2002-00079), HERMES (GOCE-CT-2005-511234-1), HERMIONE (FP7-ENV-2008-1-226354) and SESAME, by Spanish projects HIVERN (MAR98-0932), EFLUBIO (REN2002-04151-C02-01/MAR) and FAMOSO (CTM2008-06261-C03-00) and by French projects MISTRALS-MERMEX and LEFE CYBER. Mikhail Emelianov work was funded by contract 2009SGR378. The authors wish to acknowledge Mireno Borghini, Gian Pietro Gasparini, Claudie Marec and Louis Prieur for some of the CTD data acquisition and processing.

## Figure Captions

Figure 1. Map of the Gulf of Lions area showing the regions of dense water formation on the shelf and in the MEDOC region (striped areas) and a schematic diagram depicting the dense shelf water cascading and open sea convection processes across the margin with the water masses involved (see Table 1).

Figure 2. Long-term time series of near-bottom (30 m above seabed) and mid-water (470 m depth) temperature measured at 1000 m depth in the Lacaze-Duthiers Canyon since October 1993 plotted together with near-bottom temperature collected during winter 2005 (at 750 m depth) and winter 2006 (at 1000 m depth) in the neighbor Cap de Creus Canyon.

Figure 3. Comparison of xs-SSC profiles recorded during FAMOSO-1 cruise using simultaneously a WET Labs C-Star light transmissometer and a Seapoint optical backscatter sensor. Both signals were converted into xs-SSC using the calibrations derived by Guillén et al. (2000). See CTD cast location in Figure 4b at 41° 34.33'N; 5° 1.38'E.

Figure 4. Map from the western Mediterranean (a) showing the location of the compiled CTD casts with dots in a color code for each year considered in this study and the position of the long-term mooring (star) at 1000 m depth in the Lacaze-Duthiers Canyon. GoL: Gulf of Lions; CM: Catalan Margin; VV: Valencia Valley; SWMB: South Western Mediterranean Basin; NWMB: North Western Mediterranean Basin; LS: Ligurian Sea. Zoom of the northwestern Mediterranean margin (b) pointing out to the CTDs illustrated in the following Figures.

Figure 5. Potential temperature, Practical Salinity and xs-SSC profiles conducted on 4 April 1998, during the FETCH-98 cruise, in the Gulf of Lions continental rise showing the four water masses found in this region (Table 1) and the absence of BNL. See CTD cast location in Figure 4b at 42° 9.74'N; 4° 51.33'E.

Figure 6. Potential temperature, Practical Salinity and xs-SSC profiles conducted on 21 February 1999, during the HIVERN-99 cruise, in the Catalan continental rise. See CTD cast location in Figure 4b at 41° 23.01'N; 3° 47.75'E.

Figure 7. Potential temperature, Practical Salinity and xs-SSC profiles conducted on 25 February 1999, during the HIVERN-99 cruise, in the Valencia Valley, half-way between the Catalan coast and the Balearic Islands. See CTD cast location in Figure 4b at 40° 40.42'N; 2° 53.70'E.

Figure 8. Potential temperature, Practical Salinity and xs-SSC profiles conducted on 6 February 2000, during the HIVERN-00 cruise, in the Valencia Valley, half-way between the Catalan and the Balearic margin. See CTD cast location in Figure 4b at 40° 43.07'N; 2° 50.78'E.

Figure 9. Potential temperature, Practical Salinity and xs-SSC profiles conducted on 18 September 2004, during the EFLUBIO-1 cruise, in the northwestern Mediterranean basin. See CTD cast location in Figure 4b at 41° 42.00'N; 5° 10.00'E. Note that this profile reached down to 2000 m depth and that the seafloor was located at ~2400 m depth.

Figure 10. Potential density and xs-SSC profiles conducted in four CTD stations across the Catalan margin off Barcelona on 24 March 2005, during the EFLUBIO-2 cruise. See hydrographic transect location in Figure 4b.

Figure 11. Potential temperature, Practical Salinity and turbidity xs-SSC conducted on 29 March 2005, during the EFLUBIO-2 cruise, in the northwestern Mediterranean basin. See CTD cast location in Figure 4b at 41° 41.97'N; 4° 59.03'E. Note that this profile reached down to 2000 m depth and that the seafloor was located at ~2400 m depth.

Figure 12. Potential temperature, Practical Salinity and turbidity xs-SSC conducted on 26 April 2005, during the STRATA-3 cruise, at the mouth of the Cap de Creus Canyon. See CTD cast location in Figure 4b at 42° 14.85'N; 4° 20.63'E.



Figure 13. Potential temperature, Practical Salinity and xs-SSC profiles conducted on 23 April 2006, during the HERMES-3 cruise, in the MEDOC region. See CTD cast location in Figure 4b at 42° 05.00'N; 4° 40.00'E.

Figure 14. Potential temperature, Practical Salinity and xs-SSC profiles conducted on 3 July 2007, during the HERMES-6 cruise, in the MEDOC region. See CTD cast location in Figure 4b at 41° 59.94'N; 4° 59.94'E.

Figure 15. Potential temperature, Practical Salinity and xs-SSC profiles conducted on 29 March 2008, during the DEEP-1 cruise, in the MEDOC region. See CTD cast location in Figure 4b at 42° 05.00'N; 4° 40.00'E.

Figure 16. Potential temperature, Practical Salinity and xs-SSC profiles conducted on 3 May 2009, during the FAMOSO-3 cruise in the Catalan continental rise. See CTD cast location in Figure 4b at 41° 29.88'N; 3° 56.46'E.

Figure 17. Potential temperature, Practical Salinity and xs-SSC profiles conducted on 16 September 2010, during the DEEP-5 cruise, in the MEDOC region. See CTD cast location in Figure 4b at 42° 01.87'N; 4° 41.85'E.

Figure 18. Potential temperature, Practical Salinity and xs-SSC profiles conducted on March 2011, during the CASCADE cruise, in the MEDOC region. See CTD cast location in Figure 4b at 42° 02.04'N; 5° 06.12'E.

Figure 19. Short-term variability of xs-SSC profiles in the MEDOC region from the same station (SC2400) reoccupied several times during the CASCADE cruise. See CTD cast location in Figure 4b at 42° 05.00'N; 4° 40.00'E. Data has been illustrated in two plots for easy visualization of the numerous profiles.

Figure 20. Profiles of FTU, BAC, large particles abundance, volumetric concentration and fluorescence in the MEDOC region from the SC2400 station (the same as in Figure 19) obtained during the CASCADE cruise in March 4, 2011 at 22:27.

Figure 21. Comparative average particle size-distribution, from (A) the UVP, (B) sonicated filtered suspended particle samples collected in the BNL at the SC2400 station during the CASCADE cruise (the same as in Figure 20), and from (C) the superficial sediment (0-0.5 cm) at the same CTD location.

Figure 22.  $\theta$ - $S_p$  diagram of two CTD casts performed during the HIVERN-99 (see Figures 6 and 7) illustrating the origin of the thermohaline “hook”.

Figure 23. Time series of  $\theta$ - $S_p$  diagrams with the xs-SSC parameter represented in color code (1998: FETCH; 1999: TRANSMED; 2000: HIVERN-00; 2004: EFLUBIO; 2005: MEDDOCC-05 and STRATA-3; 2006: MEDOCC-06; 2007: HERMES-6; 2008: DEEP-1 and DEEP-2; 2009: FAMOSO-2; 2010: DEEP-5; 2011: CASCADE).

Figure 24. Maps showing the extension of the BNL in the western Mediterranean basin after deep cascading events. Black dots represent the CTD locations (June 1999: TRANSMED and GEOTETHYS; May 2005: MEDOCC-05; June 2006: MEDOCC-06). Note that during the trans-Mediterranean cruise BOUM conducted in July 2008 (CTD locations illustrated with white dots), the BNL was still present in the entire basin.

## References

- Armi, L., 1978. Some evidence for boundary mixing in the deep ocean. *Journal of Geophysical Research* 83, 1971-1979.
- Asper, V.L. 1986. Accelerated settling of particulate matter by "marine snow" aggregates. Ph.D. Thesis. WHOI/MIT joint educational program, 189 pp.
- Asper, V.L., 1987. Measuring the flux and sinking speed of marine snow aggregates. *Deep Sea Research* 34, 1-17.
- Baker, E.T., Lavelle J.W., 1984. The effect of particle size on the light attenuation coefficient of natural suspensions. *Journal of Geophysical Research* 89, 8197-8203.
- Béthoux, J.P., Durrieu de Madron, X., Nyffeler, F., Tailliez, D., 2002. Deep water in the western Mediterranean: peculiar 1999 and 2000 characteristics, shelf formation hypothesis, variability since 1970 and geochemical inferences, *Journal of Marine Systems* 33-34, 117-131.

- Biscaye, P.E., Eittrheim, S.L., 1974. Variations in benthic boundary layer phenomena: nepheloid layer in the North American Basin. In: Gibbs, R.J. (Ed.), *Suspended solids in water*. Plenum Press, New York, pp. 227-260.
- Biscaye, P.E., Eittrheim, S. L., 1977. Suspended particulate loads and transports in the nepheloid layer of the abyssal Atlantic Ocean. *Marine Geology* 23, 155-172.
- Bishop, J.K.B., 1986. The correction and suspended particulate matter calibration of Sea Tech transmissometer data. *Deep-Sea Research* 33, 121-134.
- Bougis, P., Ruivo, M., 1954. Sur une descente des eaux superficielles en profondeur (cascading) dans le sud du Golfe du Lion. *Bulletin d'Information du Comité Central d'Océanographie et d'Etude des Côtes* 6, 147-154.
- Boss, E., Slade, W., Hill, P. 2009. Effect of particulate aggregation in aquatic environments on the beam attenuation and its utility as a proxy for particulate mass, *Optics Express*, 17(11), 9408–9420, doi:10.1364/OE.17.009408.
- Brewer, P.G., Spencer, D.W., Biscaye, P.E., Hanley, A., Sachs, P.L., Smith, C.L., Kadar, S., Fredericks, J., 1976. The distribution of particulate matter in the Atlantic Ocean. *Earth and Planetary Science Letters* 32, 393-402.
- Canals, M., Puig, P., Durrieu de Madron, X., Heussner, S., Palanques, A., Fabrès, J., 2006. Flushing submarine canyons. *Nature* 444 (7117), 354-357.
- Chu, P.C., Gascard, J.C. (Eds.), 1991. *Deep convection and deep water formation in the oceans*. Elsevier oceanography series 57, 382 pp.
- CIESM, 2009. *Dynamics of Mediterranean Deep Waters*. CIESM Workshop Monographs, 38, 132 p.
- Company, J.B., Puig, P., Sardà, F., Palanques, A., Latasa, M., Scharek, R., 2008. Climate influence on deep sea populations. *PLoS ONE* 3(1), e1431, doi:10.1371/journal.pone.0001431.
- Cooper, L.N.H., Vaux, D., 1949. Cascading over the continental slope of water from the Celtic Sea. *Journal of the Marine Biological Association of the United Kingdom* 28, 719-750.
- Downing, J. 2006. Twenty-five years with OBS sensors: The good, the bad, and the ugly. *Continental Shelf Research* 26, 2299-2318.
- Dufau-Julliand, C., Marsaleix, P., Petrenko, A., Dekeyser, I., 2004. Three-dimensional modeling of the Gulf of Lion's hydrodynamics (northwest Mediterranean) during January 1999 (MOOGLI3 Experiment) and late winter 1999: Western Mediterranean Intermediate Water's (WIW's) formation and its cascading over the shelf break. *Journal of Geophysical Research* 109, C11002.

Durrieu de Madron, X., Zervakis, V., Theocharis, A., Georgopoulos, D., 2005. Comments on "Cascades of dense water around the world ocean". *Progress in Oceanography* 64, 83-90.

Eisma, D., 1993. *Suspended matter in the Aquatic Environment*. Springer-Verlag, Berlin, 315 pp.

Eittrheim, S., Ewing, M., 1974. Turbidity distribution in the deep waters of the western Atlantic trough. In: *Suspended Solids in Water*, R.J. Gibbs (ed.), Plenum Press, New York, 213-225.

Eittrheim, S., Thorndike, E.M., Sullivan, L., 1976. Turbidity distribution in the Atlantic Ocean. *Deep Sea Research* 23, 1115-1137.

Ewing, M., Thorndike, E.M., 1965. Suspended matter in deep ocean water. *Science*, 147, 1291-1294.

Fieux, M., 1974. Formation d'eau dense sur le plateau du golfe du Lion. In: *Processus de formation des eaux profondes. Colloques Internationaux du CNRS* 215, 165-174.

Fohrmann, H., Backhaus, J.O., Blaume, F., Rumohr, J., 1998. Sediments in bottom-arrested gravity plumes: Numerical case studies. *Journal of Physical Oceanography* 28, 2250-2274.

Font, J., Salat J., Tintoré, J., 1988. Permanent features of the circulation in the Catalan Sea. *Oceanologica Acta* 9, 51-57.

Font, J., Puig, P., Salat, J., Palanques, A., Emelianov, M., 2007. Sequence of hydrographic changes in the NW Mediterranean deep water due to the exceptional winter 2005. *Scientia Marina* 72, 339-346.

Fuda, J.L., Bengara, L., Curtil, C., El Moumni, B., Font, J., Lefevre, D., Millot, C., Taupier-Letage, I., Raimbault, P., Rougier, G., Sammari, C., 2009. Recent dense water formation in the Mediterranean western basin, as observed by HYDROCHANGES. In: Briand, F. (Ed.), *Dynamics of Mediterranean Deep Waters*. CIESM Workshop Monographs 38 "", pp. 29-33.

Gardner, W.D., Walsh, I.D., 1990. Distribution of macroaggregates and fine-grained particles across a continental margin and their potential role in fluxes. *Deep Sea Research* 37, 401-411.

Gardner, W.D., Richardson, M.J., Walsh, I.D., Berglund, B.L., 1990. In-situ optical sensing of particles for determination of ocean processes: processes: what satellites can't see, but transmissometers can. *Oceanography* 3, 11-17.

Gardner, W.D., Richardson, M.J., 1992. Particle export and resuspension fluxes in the western North Atlantic. In: Rowe, G.T., Pariente, V. (Eds.), *Deep-Sea Food Chains and the Global Carbon Cycle*, NATO Advanced Research Workshop. Kluwer Academic Publishers, Netherlands, pp. 339-364.

- Gascard, J.C., 1978. Mediterranean deep water formation, baroclinic instability and oceanic eddies. *Oceanologica Acta* 1(3), 315-330.
- Gasparini, G.P., Ortona, A., Budillon, G., Astraldi, M., Sansone, E., 2005. The effect of the Eastern Mediterranean Transient on the hydrographic characteristics in the Strait of Sicily and the Tyrrhenian Sea. *Deep-Sea Research I* 52, 915-935.
- Gonzalez, E.A., Hill, P.S., 1998. A method for estimating the flocculation time of monodispersed sediment suspensions. *Deep-Sea Research I* 54, 1931-1954.
- Gorsky, G., Picheral, M., Stemmann, L., 2000. Use of the underwater video profiler for the study of aggregate dynamics in the north Mediterranean. *Estuarine, Coastal and Shelf Science* 50, 121-128.
- Gross, T.F., Williams, A.J., 1991. Characterization of deep-sea storms. *Marine Geology* 99, 281-301.
- Guillén, J., Palanques, A., Puig, P., Durrieu de Madron, X., Nyffeler, F., 2000. Field calibrations of optical sensors for measuring suspended sediment concentrations in the Western Mediterranean. *Scientia Marina* 64(4), 427-435.
- Hall, I.R., Schmidt, S., McCave, I.N., Reyss, J.-L., 2000. Particulate matter distribution and  $^{234}\text{Th}/^{238}\text{U}$  disequilibrium along the Northern Iberian Margin; Implications for particulate organic carbon export. *Deep-Sea Research I*, 47, 557-582.
- Harris, J.E., 1972. Characterisation of suspended matter in the Gulf of Mexico, 1. Spatial distribution of suspended matter. *Deep Sea Research* 19, 719-726.
- Harris, J.E., 1977. Characterisation of suspended matter in the Gulf of Mexico, 2. Particle size analysis of suspended matter from deep water. *Deep Sea Research* 24, 1055-1061.
- Herrmann, M., Sevault, F., Beuvier, J., Somot, S., 2010. What induced the exceptional 2005 convection event in the northwestern Mediterranean basin? Answers from a modeling study. *Journal of Geophysical Research* 115, C12051 [doi:10.1029/2010JC006162].
- Heussner, S., Durrieu de Madron, X., Calafat, A., Canals, M., Carbonne, J., Delsaut, N., Saragoni, G., 2006. Spatial and temporal variability of downward particle fluxes on a continental slope: Lessons from an 8-yr experiment in the Gulf of Lions (NW Mediterranean). *Marine Geology* 234, 63-92.
- Hill, P.S., Boss, E., Newgard, J.P., Law, B.A., Milligan, T.G. 2011. Observations of the sensitivity of beam attenuation to particle size in a coastal bottom boundary layer. *Journal of Geophysical Research*, 116, C02023, doi:10.1029/2010JC006539.
- Hollister, C.G., McCave, I.N., 1984. Sedimentation under deep-sea storms. *Nature* 309, 220-225.

Hollister, C.D., Nowell, A.R.M., 1991. Prologue: Abyssal storms as a global geologic process. *Marine Geology* 99, 275-280.

Houpert, L., 2010. Étude du renouvellement des eaux profondes en Méditerranée nord occidentale pendant la période 2007/2010. Msc Thesis. Université Pierre et Marie Curie, Paris, pp 63. ([http://cefrem.univ-perp.fr/files/Houpert\\_rapportM2\\_v2.pdf](http://cefrem.univ-perp.fr/files/Houpert_rapportM2_v2.pdf)).

Ivanov, V.V., Shapiro, G.I., Huthnance, J.M., Aleynik, D.L. Golovin, P.N., 2004. Cascades of dense water around the world ocean. *Progress in Oceanography* 60, 47-98.

IOC, SCOR, IAPSO, 2010. The international thermodynamic equation of seawater - 2010. Calculations and use of thermodynamic properties. Intergovernmental Oceanographic Commission. Manual and Guides N° 56, UNESCO, 196 pp.

Jerlov, N.G., 1953. Particle distribution in the ocean. Reports of the Swedish Deep Sea Expedition 3, 73-97.

Jerlov, N.G., 1968. *Optical oceanography*, Elsevier, New York, 194 pp.

Kalle, K., 1937. Nährstoff-Untersuchungen als hydrographisches Hilfsmittel zur Unterscheidung von Wasserkörpern. *Annalen der Hydrographie und Maritimen Meteorologie* 65, 1-18.

Killworth, P.D., 1976. The mixing and spreading phases of MEDOC I. *Progress in Oceanography* 7, 59-90.

Killworth, P.D., 1983. Deep convection in the world ocean. *Reviews of Geophysics and Space Physics* 21(1), 1-26.

Kolla, V., Sullivan, L., Streeter, S.S., Langseth, M.G., 1976. Spreading of Antarctic Bottom water and its effects on the floor of the Indian Ocean inferred from bottom water potential temperature, turbidity and seafloor photography. *Marine Geology* 21, 171-189.

Kolla, V., Henderson, L., Sullivan, L., Biscaye, P.E., 1978. Recent sedimentation in the southeast Indian Ocean with special reference to the effects of Antarctic Bottom Water circulation. *Marine Geology* 27, 1-17.

Lacombe, H., 1992. General physical oceanography of the Mediterranean Sea. In Charnock, H. (Ed.), *Winds and currents of the Mediterranean basin*. Reports in Meteorology and Oceanography, 40. Harvard University, pp. 39-73.

Lacombe, H., Tchernia, P., 1974. Évolution hydrologique dans la zone de formation d'eau profonde au large de la côte méditerranéenne française par hiver très froid (1962-1963). In: *Processus de formation des eaux profondes*. Colloques Internationaux du CNRS 215, 191-201.

Lacombe, H., Tchernia, P., 1974. Les zones de formation d'eau profonde océanique, caractères, processus, problèmes. In: *Processus de formation des eaux profondes*. Colloques Internationaux du CNRS 215, 249-262.

- Lacombe, H., Tchernia, P., Gamberoni, L., 1985. Variable bottom water in the Western Mediterranean basin. *Progress in Oceanography* 14, 319-338.
- Lal, D., 1977. The oceanic microcosm of particles. *Science*, 198, 997-1009.
- Lapouyade, A., Durrieu de Madron, X., 2001. Seasonal variability of the advective transport of particulate matter and organic carbon in the Gulf of Lion (NW Mediterranean). *Oceanologica Acta* 24, 295-312.
- Lopez-Jurado, J.L., González-Pola, C., Vélez-Belchí, P., 2005. Observation of an abrupt disruption of the long-term warming trend at the Balearic Sea, western Mediterranean Sea, in summer 2005. *Geophysical Research Letters* 32, L24606.
- Marshall, J., Schott, F., 1999. Open ocean deep convection: observations, models and theory. *Review of Geophysics* 37, 1-64.
- Martín, J., Miquel, J.C., Khripounoff, A., 2010. Impact of open sea deep convection on sediment remobilization in the western Mediterranean. *Geophysical Research Letters* 37, L13604 [doi:10.1029/2010GL043704].
- McCave, I.N., 1983. Particulate size spectra, behaviour and origin of nepheloid layers over the Nova Scotian Continental Rise. *Journal of Geophysical Research* 88, 7647-7666.
- McCave, I.N., 1986. Local and global aspects of the bottom nepheloid layers in the World Ocean. *Netherlands Journal of Sea Research* 20(2/3), 167-181.
- MEDAR Group, 2002. Mediterranean and Black Sea Database of Temperature, Salinity and Biochemical Parameters and Climatological Atlas [CD-ROM], Inst. Fr. de Rech. pour l'Exploit. de la Mer, Plouzane, France. (Available at <http://www.ifremer.fr/sismer/program/medar/>)
- MEDOC Group, 1970. Observation of formation of deep water in the Mediterranean Sea, 1969. *Nature* 227, 1037-1040.
- Mertens, C., Schott, F., 1998. Interannual variability of deep-water formation in the northwestern Mediterranean. *Journal of Physical Oceanography* 28, 1410-1424.
- Mikkelsen, O.A., Hill, P.S., Milligan, T.G., 2006. Single-grain, microfloc and macrofloc volume variations observed with a LISST-100 and a digital floc camera. *Journal of Sea Research* 55, 87-102.
- Milligan, T.G., Hill, P.S., Law, B.A., 2007. Flocculation and the loss of sediment from the Po River plume. *Continental Shelf Research* 27, 309-321.
- Millot, C., 1985. Evidence of a several-day propagating wave. *Journal of Physical Oceanography* 15, 258-272.

- Millot, C., 1987. Circulation in the Western Mediterranean Sea. *Oceanologica Acta* 10, 143-149.
- Millot, C.A., 1990. The Gulf of Lions' hydrodynamic. *Continental Shelf Research* 10, 885-894.
- Moutin, T., Van Wambeke, F., Prieur, L., 2011. The Biogeochemistry from the Oligotrophic to the Ultraoligotrophic Mediterranean (BOUM) experiment. *Biogeosciences Discussion*, 8, 8091-8160.
- Nansen, F., 1906. Northern Waters: Captain Roald Amundsen's oceanographic observations in the Arctic Seas in 1901. In: *VidenskabsSelskabets. Skrifter, I. Matematisk-Naturv. Klasse 3*, Dybvad, Christiania, 145 pp.
- Nansen, F., 1913. The waters of the north-eastern North Atlantic. Investigations made during the cruise of the "Frithjof", of the Norwegian Royal Navy, in July 1910. *Internationale Revue der Gesamten Hydrobiologie und Hydrographie* 4: Hydrographische Supplement, 139 pp.
- Palanques, A., Durrieu de Madron, X., Puig, P., Fabr s, J., Guill n, J., Calafat, A., Canals, M., Heussner, S., Bonnin, J., 2006. Suspended sediment fluxes and transport processes in the Gulf of Lions submarine canyons. The role of storms and dense water cascading. *Marine Geology* 234, 43-61.
- Palanques, A., Puig, P., Latasa, M., Scharek, R., 2009. Deep sediment transport induced by storms and dense shelf water cascading in the northwestern Mediterranean basin. *Deep Sea Research I* 56, 425-434.
- Palanques, A., Puig, P., Durrieu de Madron, X., Sanchez-Vidal, A., Pasqual, C., Mart n, J., Calafat, A., Heussner, S., Canals, M., 2012. Sediment transport to the deep canyons and open-slope of the western Gulf of Lions during the 2006 intense cascading and open-sea convection period. *Progress in Oceanography* (in press).
- Pasqual, C., Sanchez-Vidal, A., Z niga, D., Calafat, A., Canals, M., Durrieu de Madron, X., Puig, P., Heussner, S., Palanques, A., Delsaut, N., 2010. Flux and composition of settling particles across the continental margin of the Gulf of Lion: the role of dense shelf water cascading. *Biogeosciences* 7, 217-231.
- Person, R., 1974. Un exemple de descente des eaux superficielles du plateau continental dans un canyon du Golfe du Lion. *Colloques Internationaux du CNRS* 215, 175-189.
- Picheral, M., Guidi, L., Stemmann, L., Karl, D. M., Iddaoud, G., Gorsky, G., 2010. The Underwater Vision Profiler 5: An advanced instrument for high spatial resolution studies of particle size spectra and zooplankton. *Limnology and Oceanography: Methods* 8, 462-473.
- Puig, P., Palanques, A., Guill n, J., Garc a-Ladona, E., 2000. Deep slope currents and suspended particle fluxes in and around the Foix submarine canyon (NW Mediterranean). *Deep-Sea Research I* 47, 343-366.



Puig, P., Palanques, A., Orange, D.L., Lastras, G., Canals, M., 2008. Dense shelf water cascading and furrows formation in the Cap de Creus Canyon, northwestern Mediterranean Sea. *Continental Shelf Research* 28, 2017-2030.

Puig, P., Palanques, A., Font, J., Salat, J., Latasa, M., Scharek, R., 2009. Interactions between open sea convection and shelf cascading dense waters in the formation of the Western Mediterranean Deep Water. In: Briand, F. (Ed.), *Dynamics of Mediterranean Deep Waters*. CIESM Workshop Monographs 38, pp. 81-89.

Ribó, M., Puig, P., Palanques, A., Lo Iacono, C., 2011. Dense shelf water cascades in the Cap de Creus and Palamós submarine canyons during winters 2007 and 2008. *Marine Geology* 284, 175-188.

Salat, J., Emelianov, M., Lopez-Jurado, J.L., 2006. Unusual extension of Western Mediterranean deep water formation during winter 2005. *Proceedings 5<sup>a</sup> Asamblea Hispano-Portuguesa de Geodesia y Geofísica*. [CD-ROM], Universidad de Sevilla, Sevilla, Spain.

Salat, J., Emelianov, M., Puig, P., 2009. From Bottom Water (Lacombe, 1985) to New-WMDW from 2005 onwards. Possible shifts on Open Sea Deep Convection. In: Briand, F. (Ed.), *Dynamics of Mediterranean Deep Waters*. CIESM Workshop Monographs 38, pp. 41-49.

Salat, J., Puig, P., Latasa, M., 2010. Violent storms within the Sea: dense water formation episodes in the NW Mediterranean. *Advances in Geosciences*. 26, 53-59.

Sánchez-Vidal, A., Pascual, C., Kerhervé, P., Calafat, A., Heussner, S., Palanques, A., Durrieu de Madron, X., Canals, M., Puig, P., 2008. Impact of dense shelf water cascading on the transfer of organic matter to the deep western Mediterranean basin. *Geophysical Research Letters* 35, L05605.

Sankey, T., 1973. The formation of deep water in the north-western Mediterranean. *Progress in Oceanography* 6, 159-179.

Schroeder, K., Gasparini, G.P., Tangherlini, M., Astraldi, M., 2006. Deep and intermediate water in the western Mediterranean under the influence of the Eastern Mediterranean Transient. *Geophysical Research Letters* 33, L21607.

Schröder, K., Ribotti, A., Borghini, M., Sorgente, R., Perilli, A., Gasparini, G.P., 2008. An extensive western Mediterranean deep water renewal between 2004 and 2006. *Geophysical Research Letters* 35, L18605.

Schroeder, K., Josey, S.A., Herrmann, M., Grignon, L., Gasparini, G.P., Bryden, H.L., 2010. Abrupt warming and salting of the Western Mediterranean Deep Water: Atmospheric forcings and lateral advection. *Journal of Geophysical Research* 115, C08029 [doi:10.1029/2009JC005749].

Smith, R.O., Bryden, H.L., Stansfield, K., 2008. Observations of new Western Mediterranean Deep Water formation using Argo floats 2004–2006, *Ocean Science* 4, 133-149.

Spinrad, R., Zaneveld, J.R.V., 1982. An analysis of the optical features of the near-bottom and bottom nepheloid layers in the area of the Scotian Rise. *Journal of Geophysical Research* 87, 9533-9561.

Stabholz M., Durrieu de Madron, X., Khripounoff, A., Canals, M., Taupier-Letage, I., Testor, P., Heussner, S., Kerhervé, P., Houpert, L., Delsaut, N., 2012. Impact of open-sea convection on particulate fluxes and sediment dynamics in the deep basin of the Gulf of Lions. *Biogeosciences Discussions*, 9, 12845–12894

Stommel, H., 1972. Deep winter-time convection in the western Mediterranean Sea. In: Gordon, A.L. (Ed.), *Studies in Physical Oceanography*, Vol. 2. . Gordon and Breach, New York, pp. 207-218.

Testor, P., Gascard, J.C., 2003. Large-scale spreading of Deep Waters in the western Mediterranean Sea by submesoscale coherent eddies. *Journal of Physical Oceanography* 33, 75-87.

Testor, P., Gascard, J.C., 2006. Post-convection spreading phase in the Northwestern Mediterranean Sea. *Deep-Sea Research I* 53, 869-893.

Trent, J.D. 1985. A study of macroaggregates in the marine environment. Ph.D. Thesis. University of California, 234 pp.

Ulses, C., Estournel, C., Puig, P., Durrieu de Madron, X., Marsaleix, P., 2008. Dense shelf water cascading in the northwestern Mediterranean during the cold winter 2005. Quantification of the export through the Gulf of Lion and the Catalan margin. *Geophysical Research Letters* 35, L07610 [doi:10.1029/2008GL033257].

Vangriesheim A., Gouillou, J.P., Prieur L., 1992. A deep-ocean nephelometer to detect bottom and intermediate nepheloid layers. *Deep-Sea Research* 39, 1403-1416.

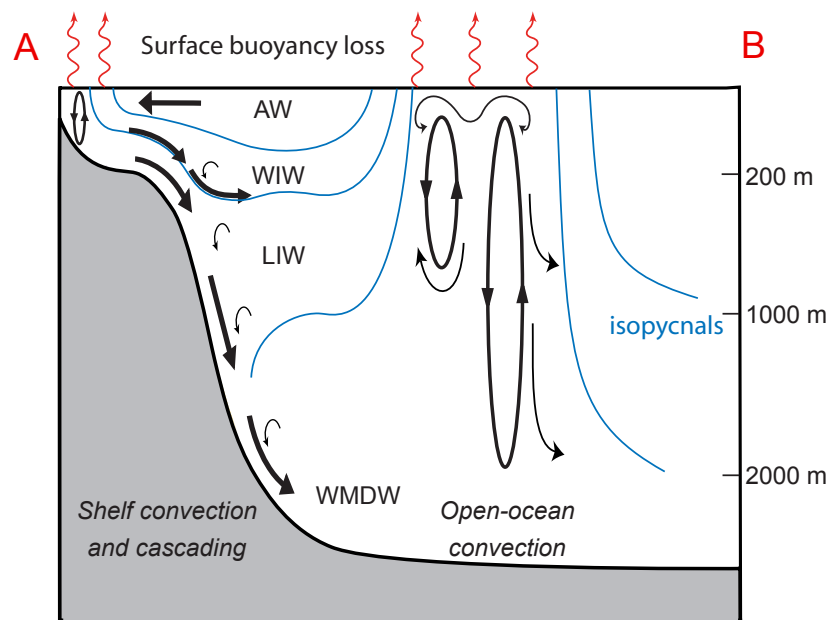
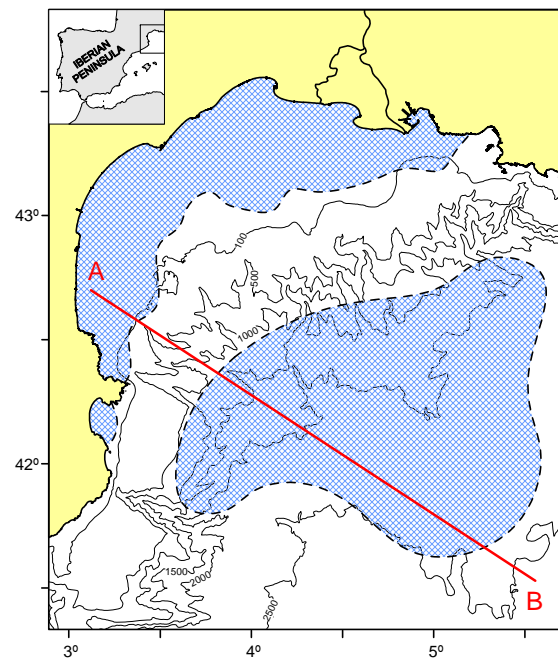
<b>Acronym</b>	<b><math>\theta</math> (°C)</b>	<b><math>S_P</math></b>	<b><math>\sigma_\theta</math> (kg/m<sup>3</sup>)</b>
"recent" AW	>13	<37.2	<28.1
"old" AW	> 13	38.0-38.2	< 28.9
WIW	12.6-13.0	38.1-38.3	28.9-29.0
LIW	13.0-13.4	38.48-38.55	29.075
WMDW	12.75-12.82	38-43-38.47	29.115-29.120

**Table 1.** Acronyms and physical characteristic of the water masses found in the northwestern Mediterranean

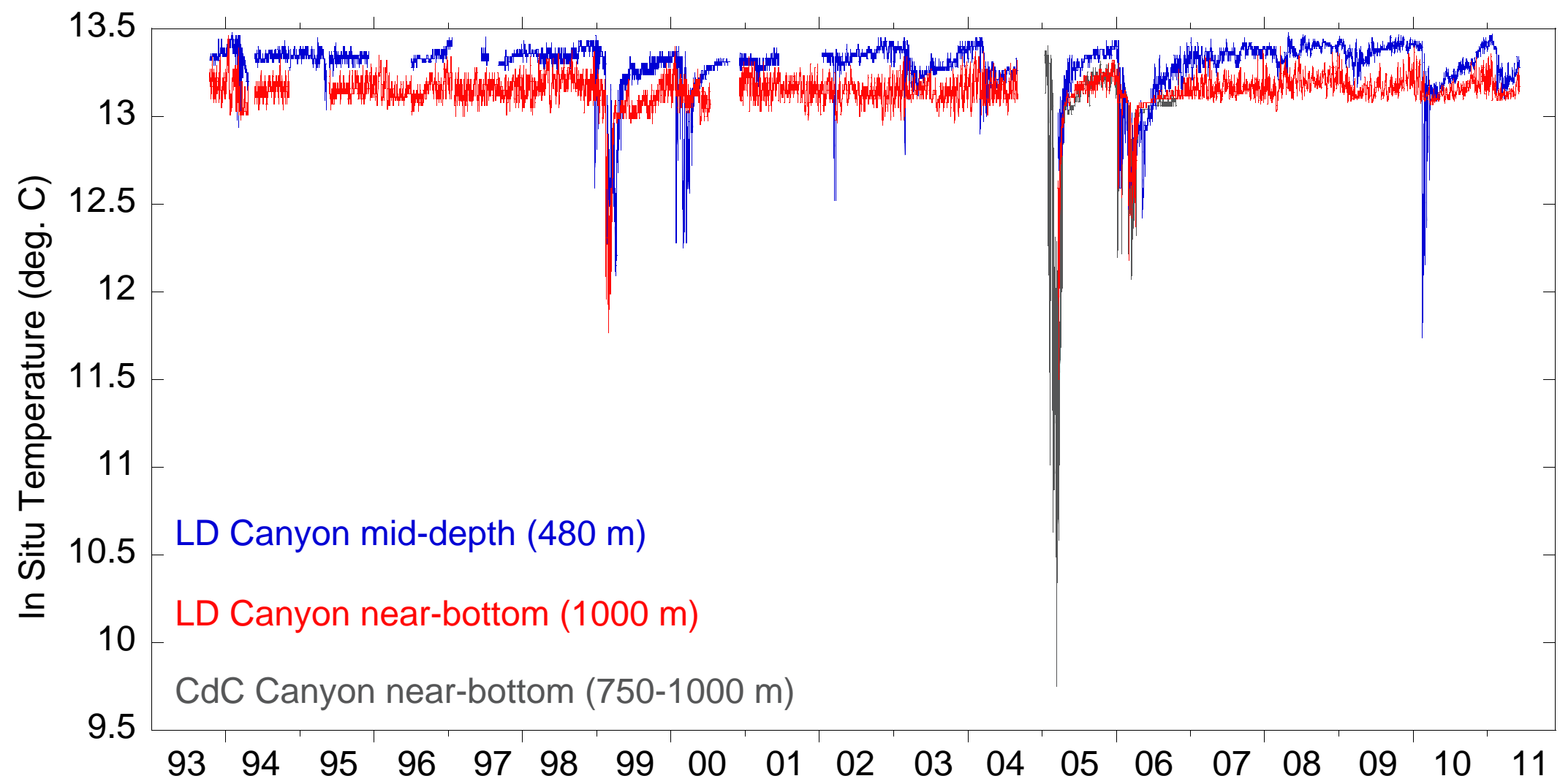
<b>Year</b>	<b>Cruise</b>	<b>Dates</b>	<b>Turbidity sensor(s)</b>
1998	FETCH	4-15 April	Sea Tech transmissometer (25 cm)
<b>1999</b>	HIVERN-99	21-25 February	Sea Tech transmissometer (20 cm)
	TRANSMED	27 June-04 July	Sea Tech transmissometer (10 cm)
	GEOTETHIS	15-17 June	Nephelometer (*)
2000	HIVERN-00	25 January-5 February	Sea Tech transmissometer (20 cm)
2004	EFLUBIO-1	14-21 September	Seapoint OBS
<b>2005</b>	EFLUBIO-2	16 March-6 April	Seapoint OBS
	GYROSCOPE	13 April	C-Star transmissometer (25 cm)
	STRATA-3	26 April	C-Star transmissometer (25 cm)
	MEDOCC-05	25 April-5 May	C-Star transmissometer (25 cm)
	TUNIBAL	12-18 July	Seapoint OBS
	CIRBAL	25 September	Seapoint OBS
	HERMES-1	17 October	C-Star transmissometer (25 cm)
<b>2006</b>	HERMES-3	23 April	C-Star transmissometer (25 cm)
	MEDOCC-06	17-28 June	C-Star transmissometer (25 cm)
	HERMES-4	16 August	C-Star transmissometer (25 cm)
2007	HERMES-6	3 July	Sea Tech transmissometer (25 cm)
2008	DEEP-1	29-30 March	Seapoint OBS
	BOUM	10-18 July	C-Star transmissometer (25 cm)
	DEEP-2	21 September	Seapoint OBS
2009	FAMOSO-1	1 February	Seapoint OBS & C-Star transmissometer (25 cm)
	DEEP-3	6 April	Seapoint OBS
	FAMOSO-2	29 April-3 May	Seapoint OBS & C-Star transmissometer (25 cm)
	42N5E	7-10 July	C-Star transmissometer (25 cm)
	DEEP-4	27 October	Seapoint OBS
2010	DEEP-5	16 September	Seapoint OBS & C-Star transmissometer (25 cm)
2011	CASCADE	4-22 March	Seapoint OBS & C-Star transmissometer (25 cm)

**Table 2.** List of the CTD data used in this study showing the year of the hydrographic cruises, its acronyms, the survey dates and the type of commercial turbidity sensor(s) coupled to the CTD probe. \*Prototype nephelometer (Vangriesheim et al., 1992). Years in bold correspond to winters with deep dense shelf water cascading (see Figure 2).

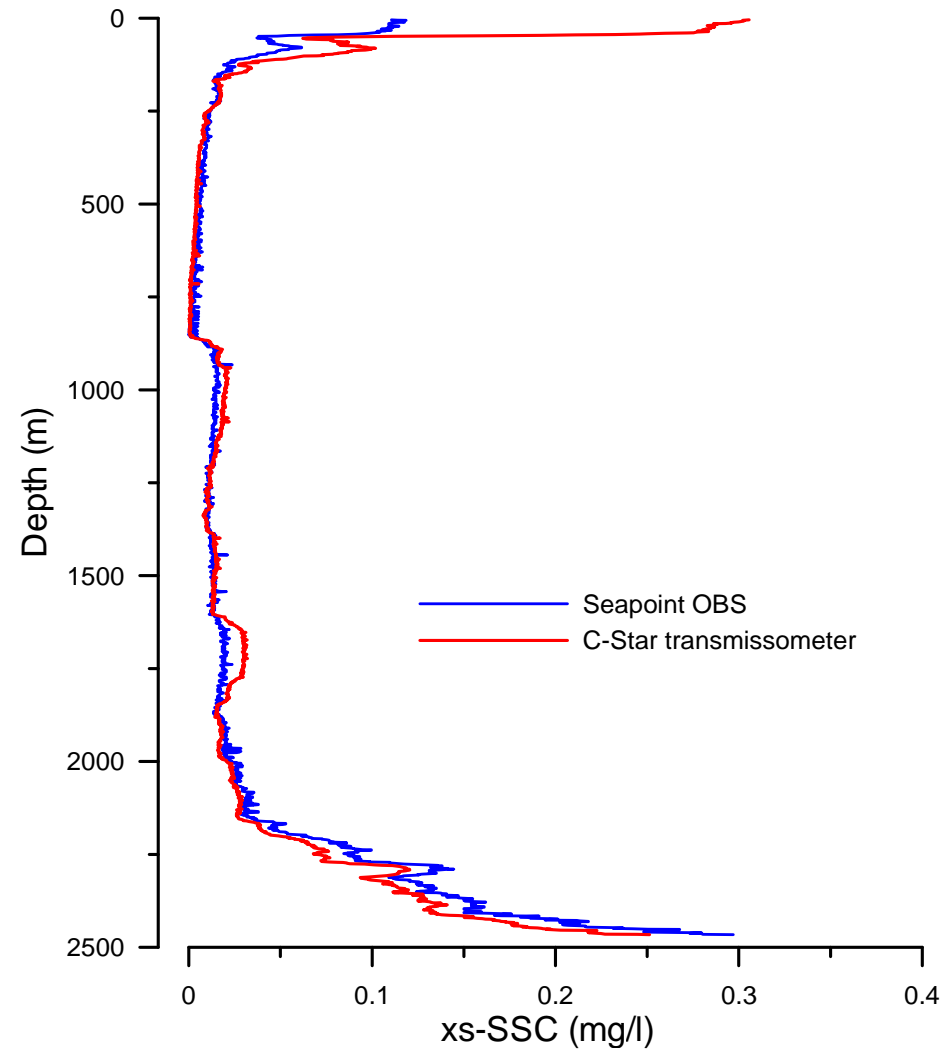
Figure



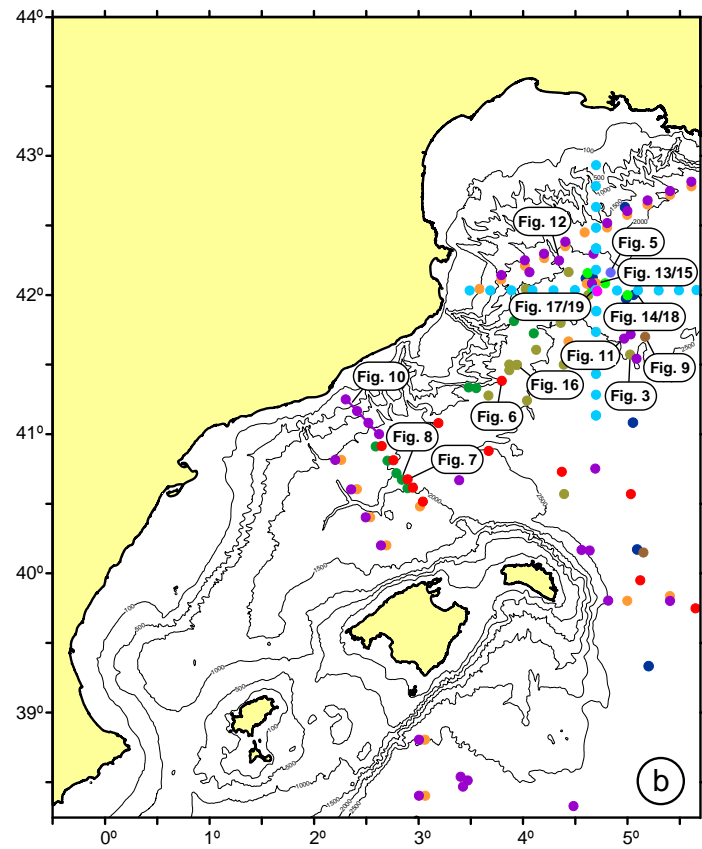
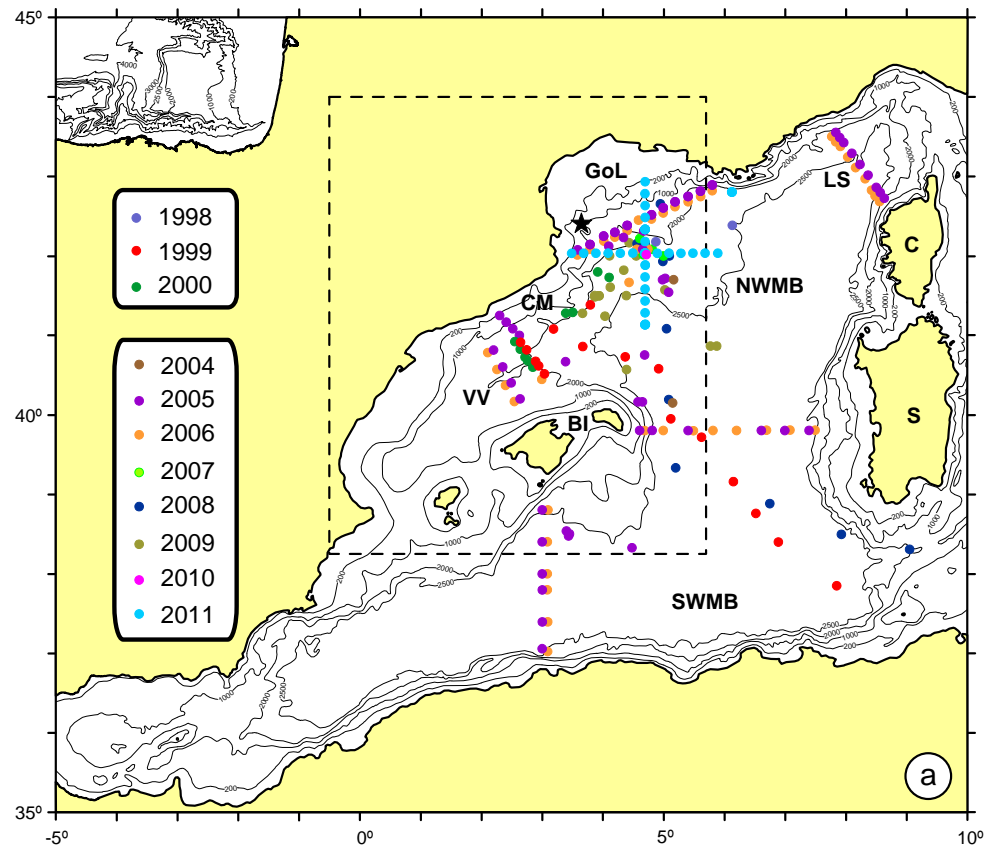
Figure



Figure

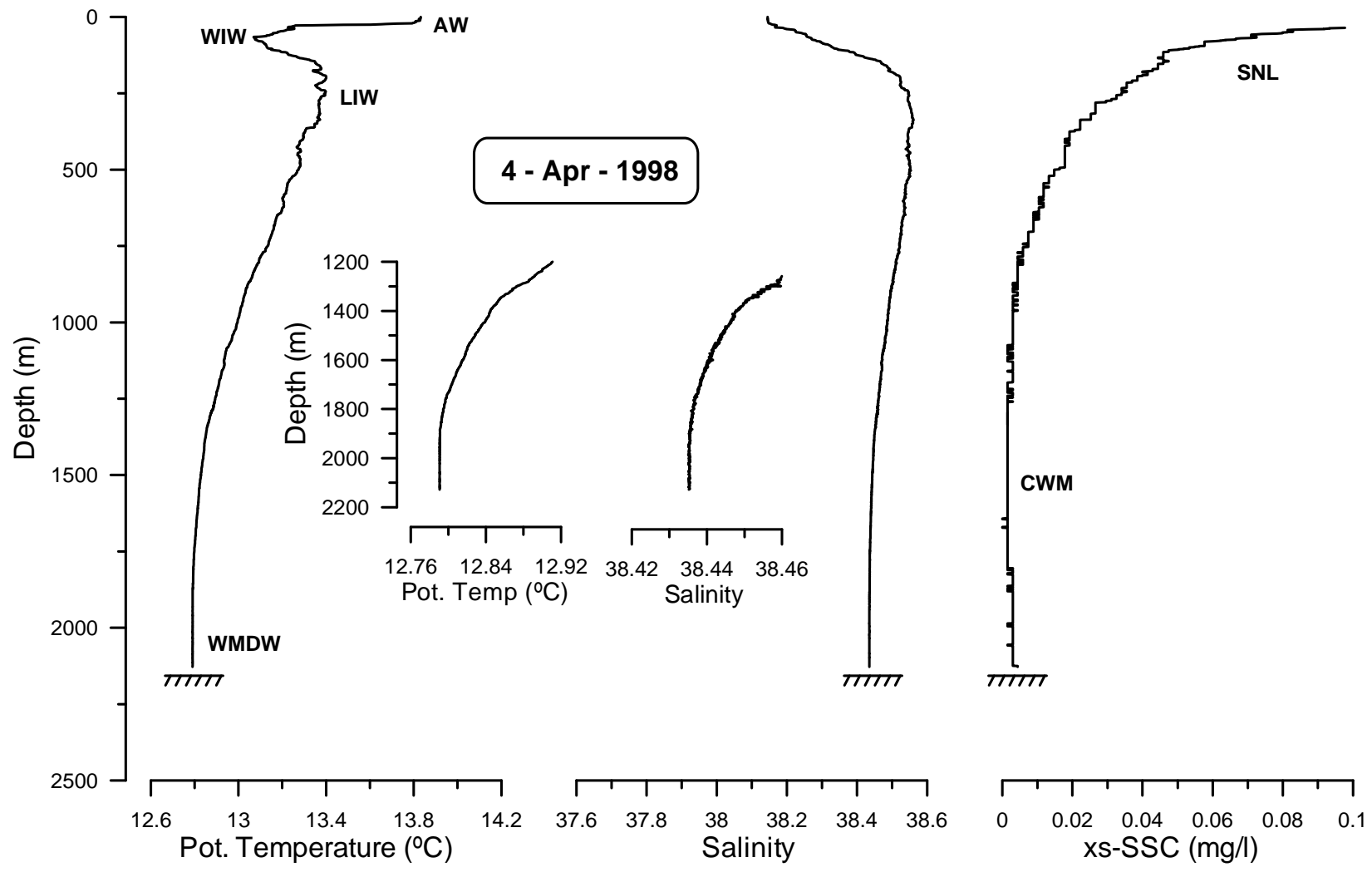


Figure

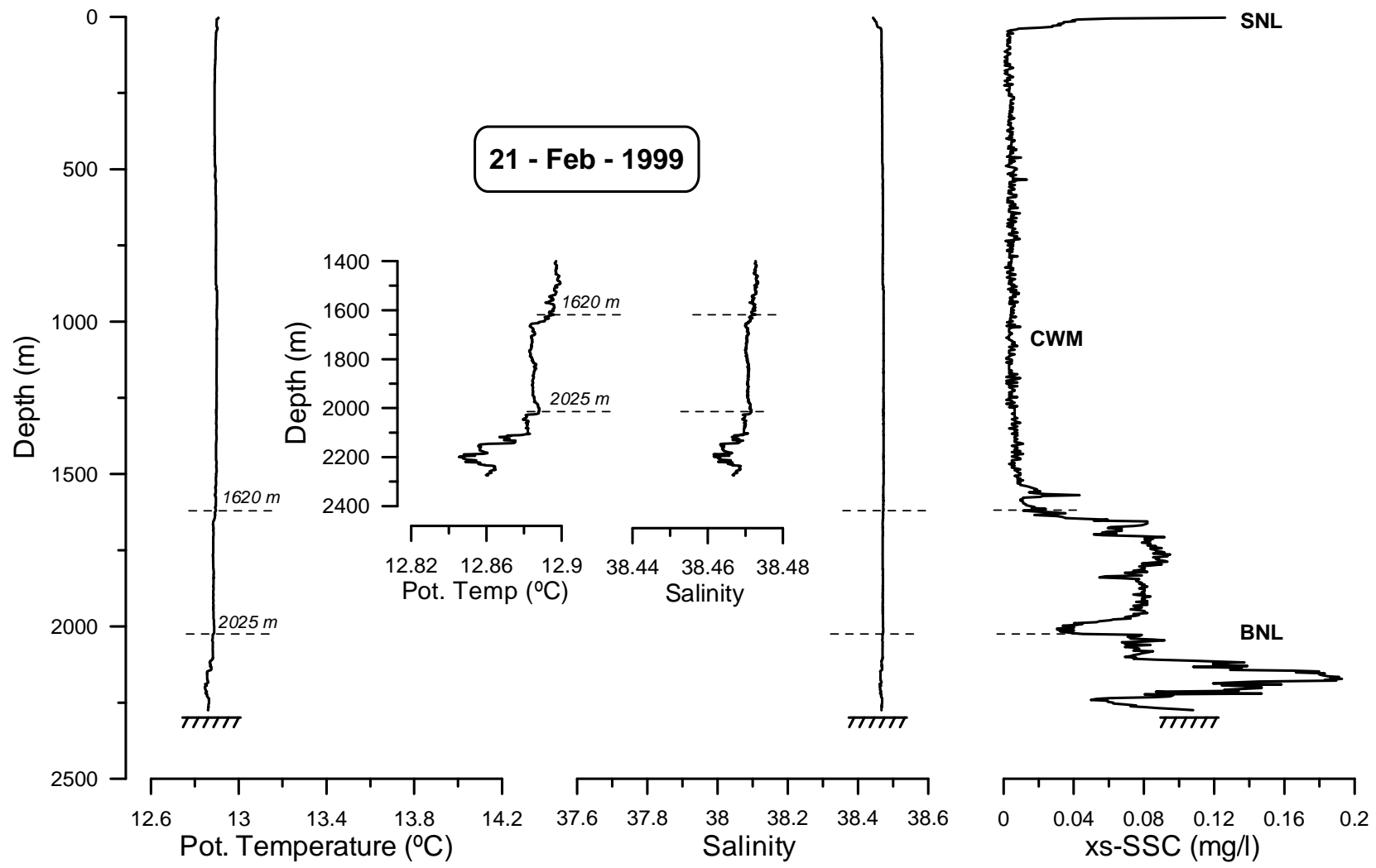




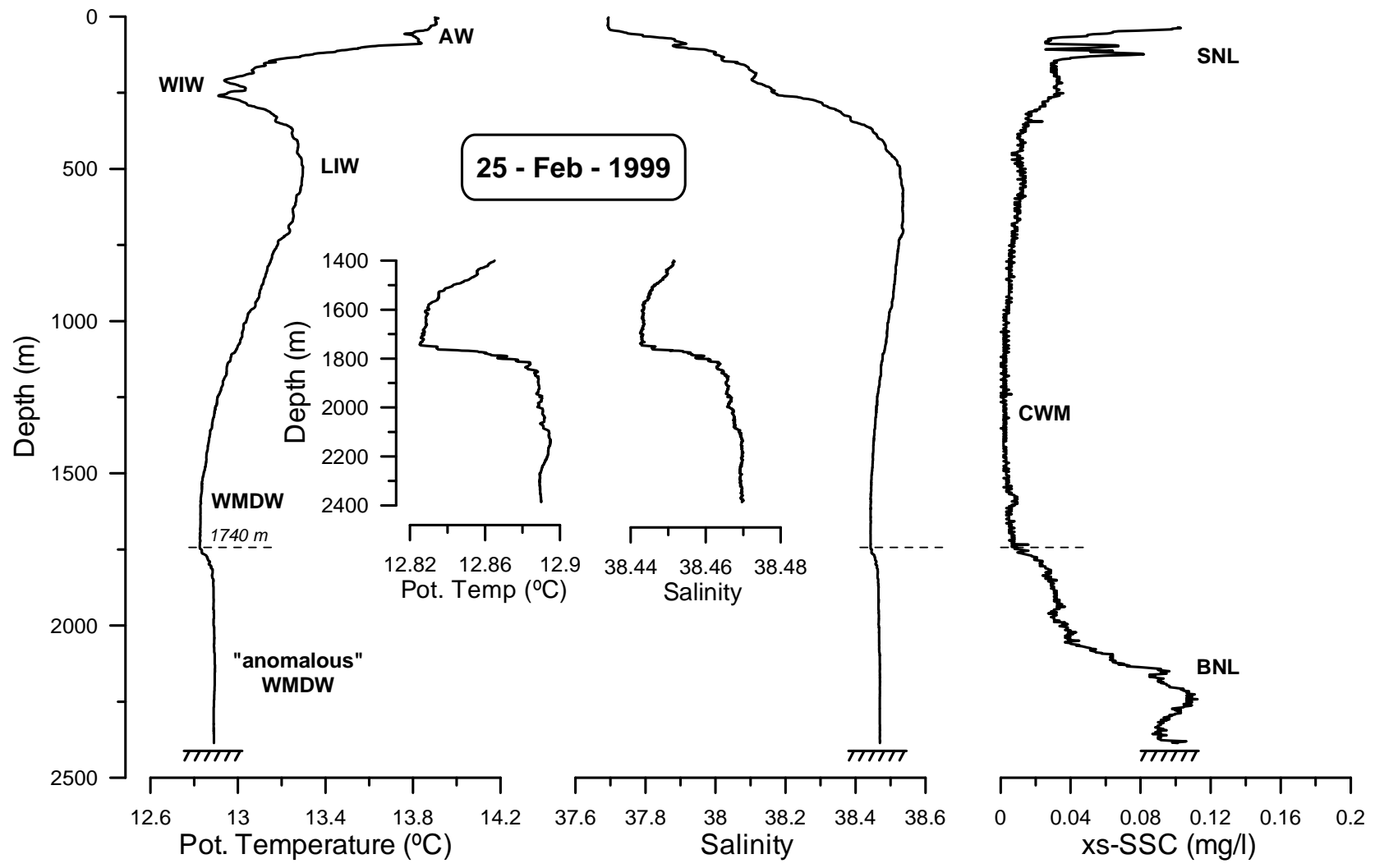
Figure



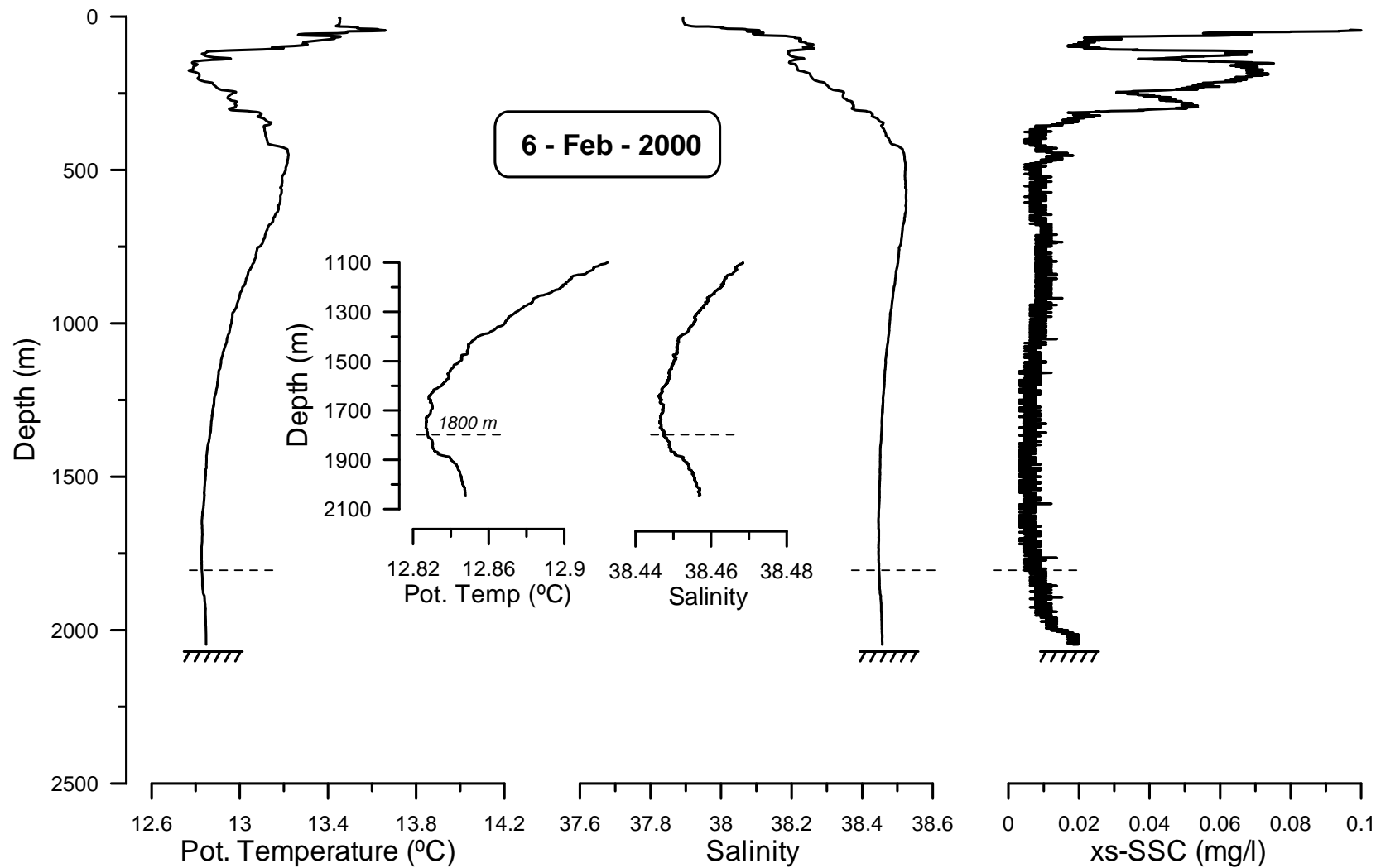
Figure



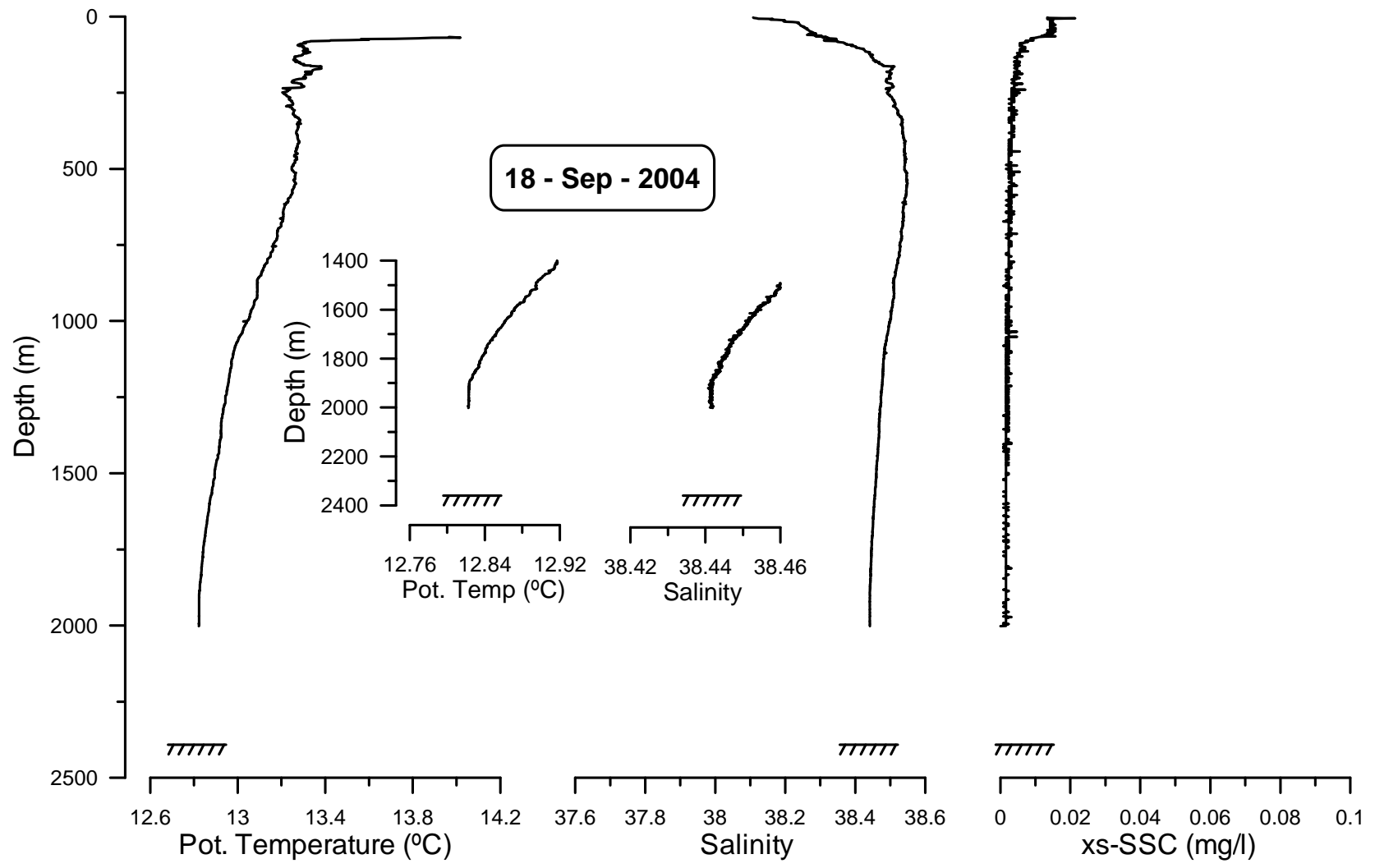
Figure



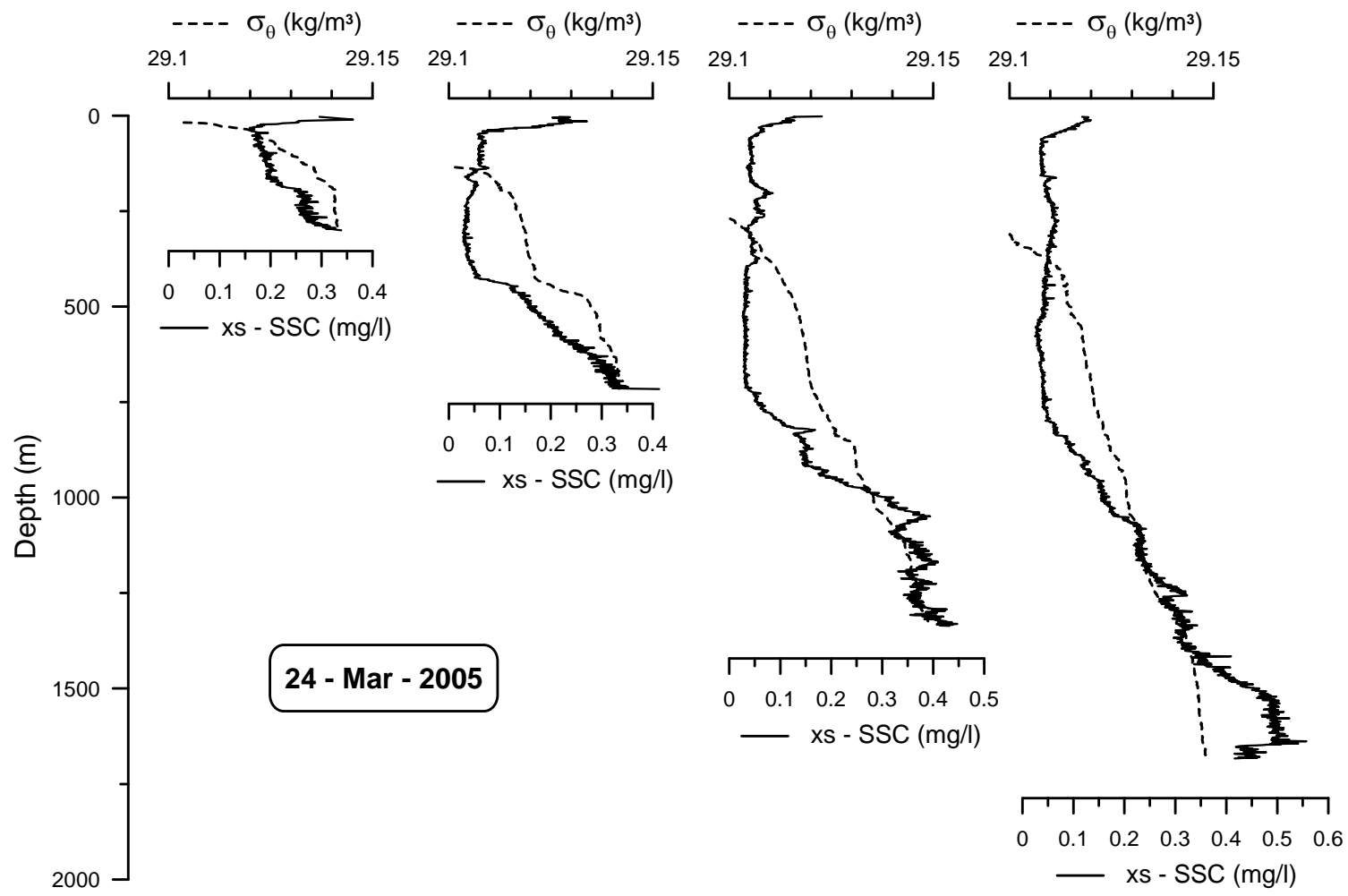
Figure



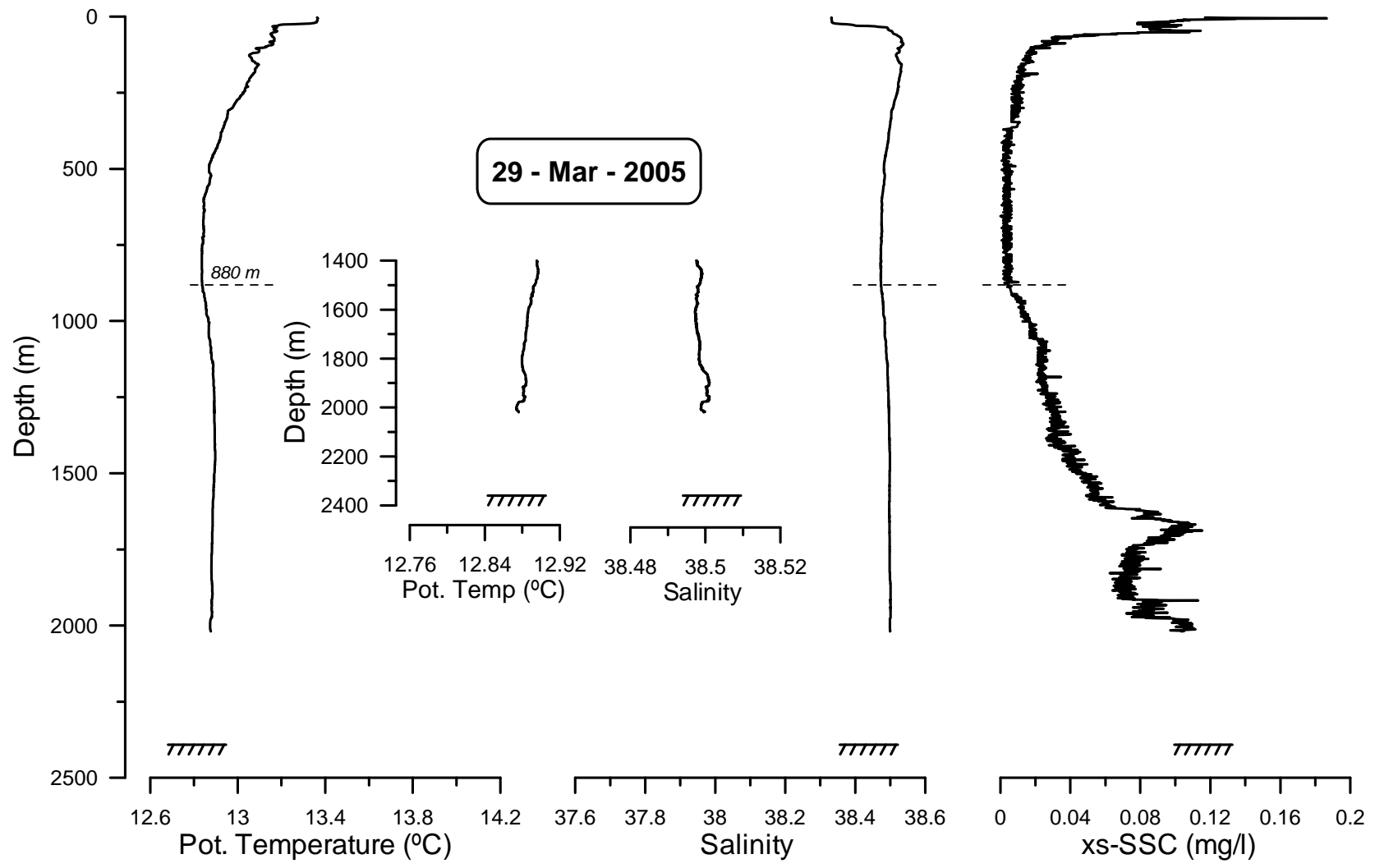
Figure



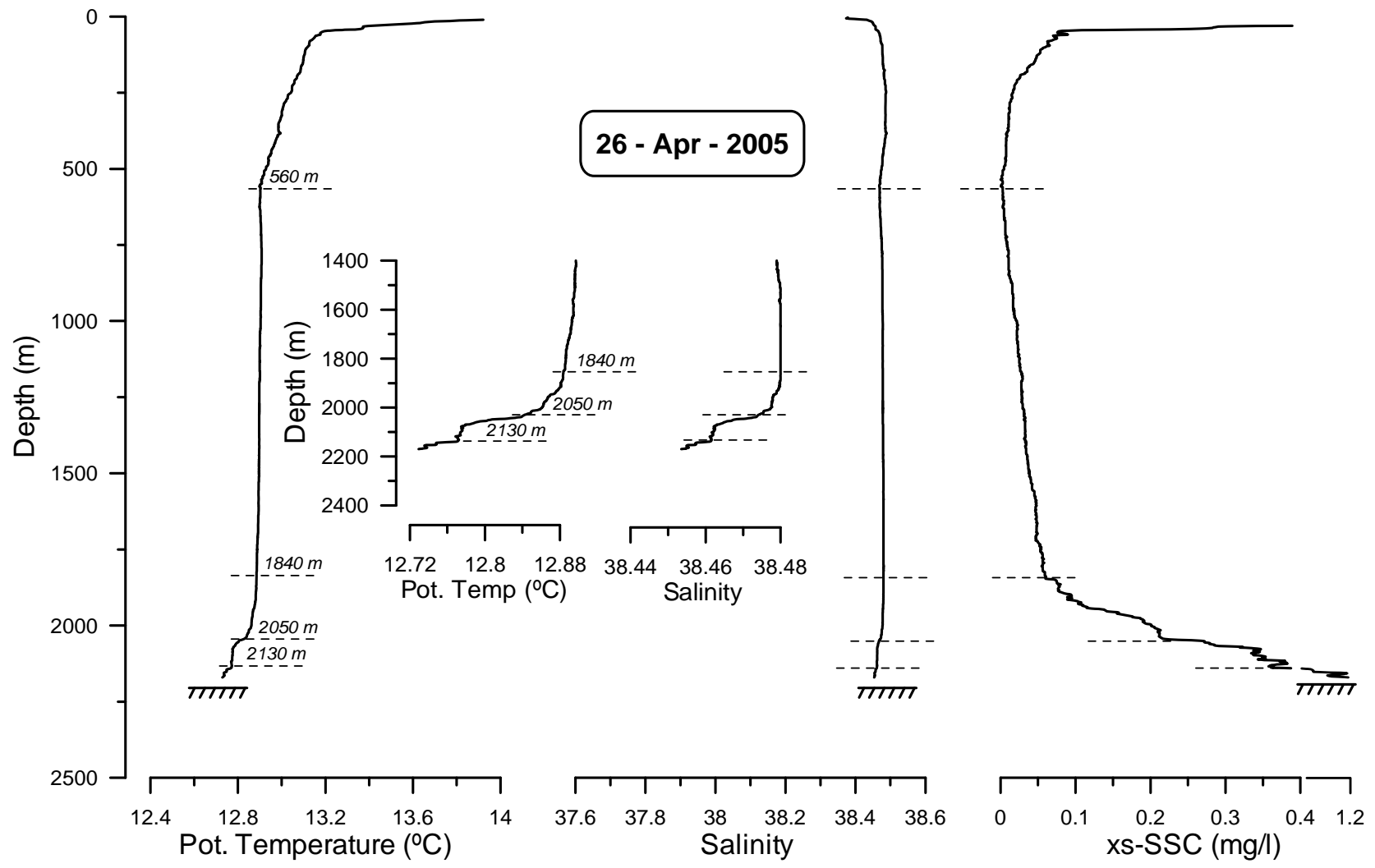
Figure



Figure

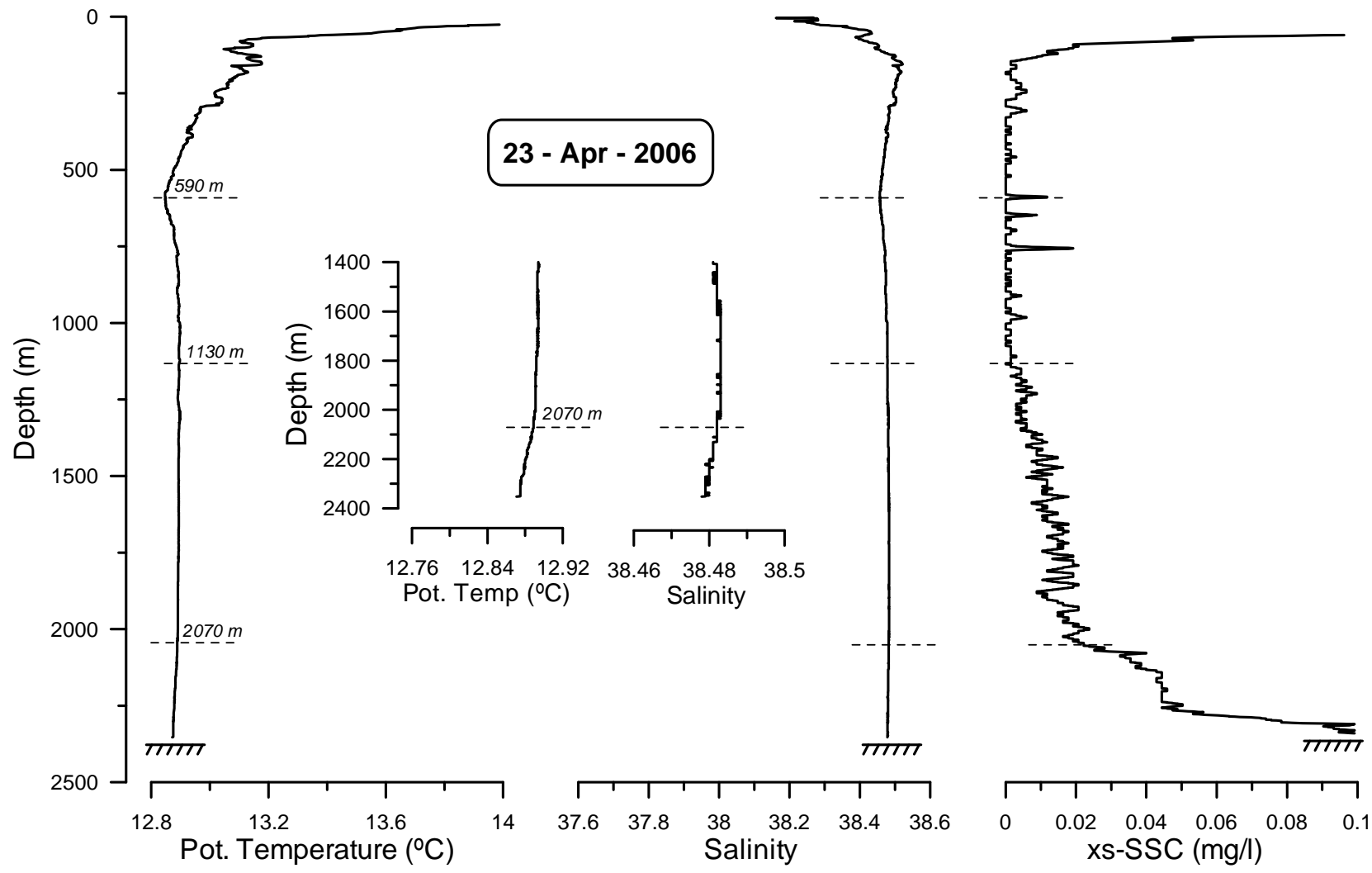


Figure

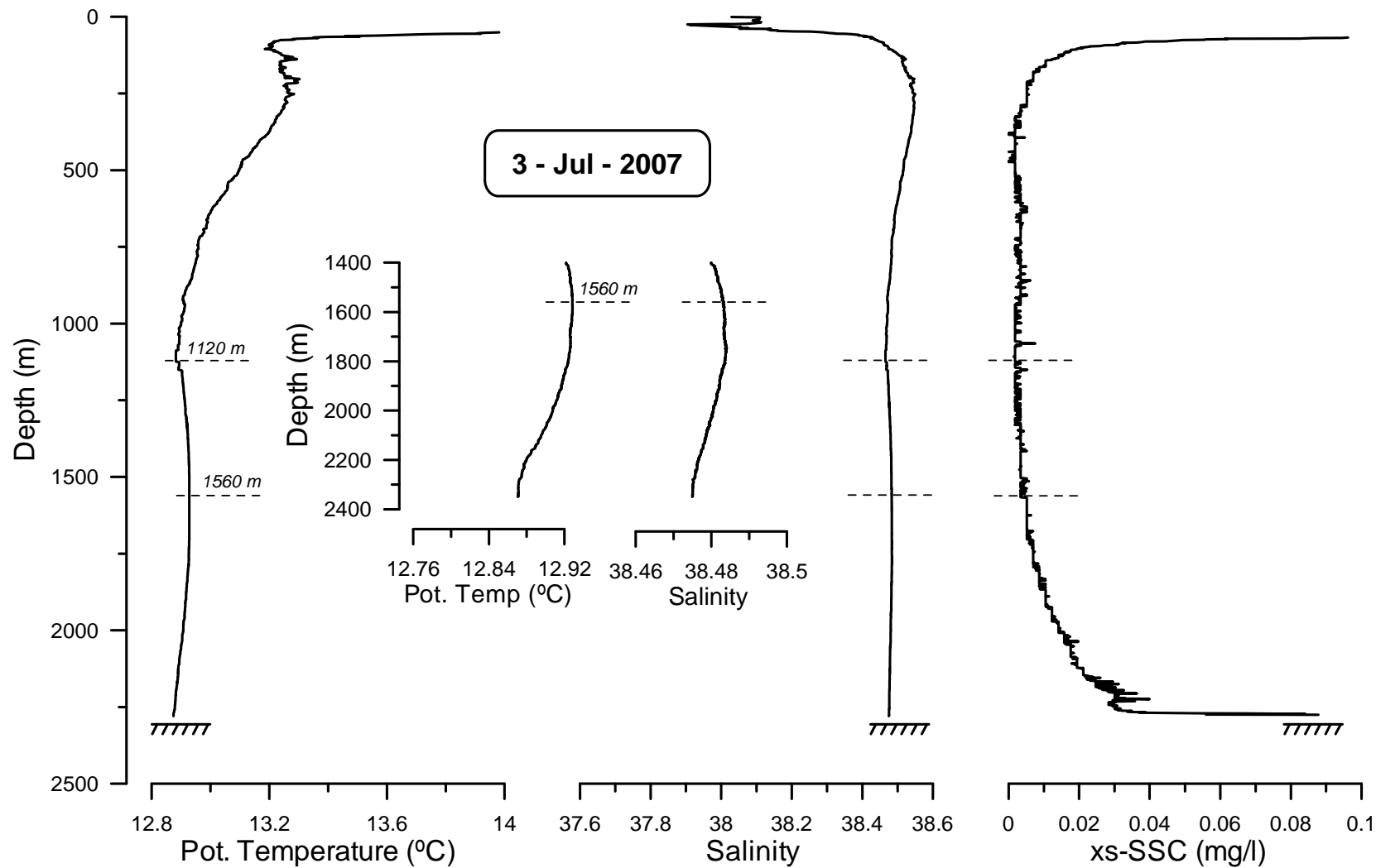




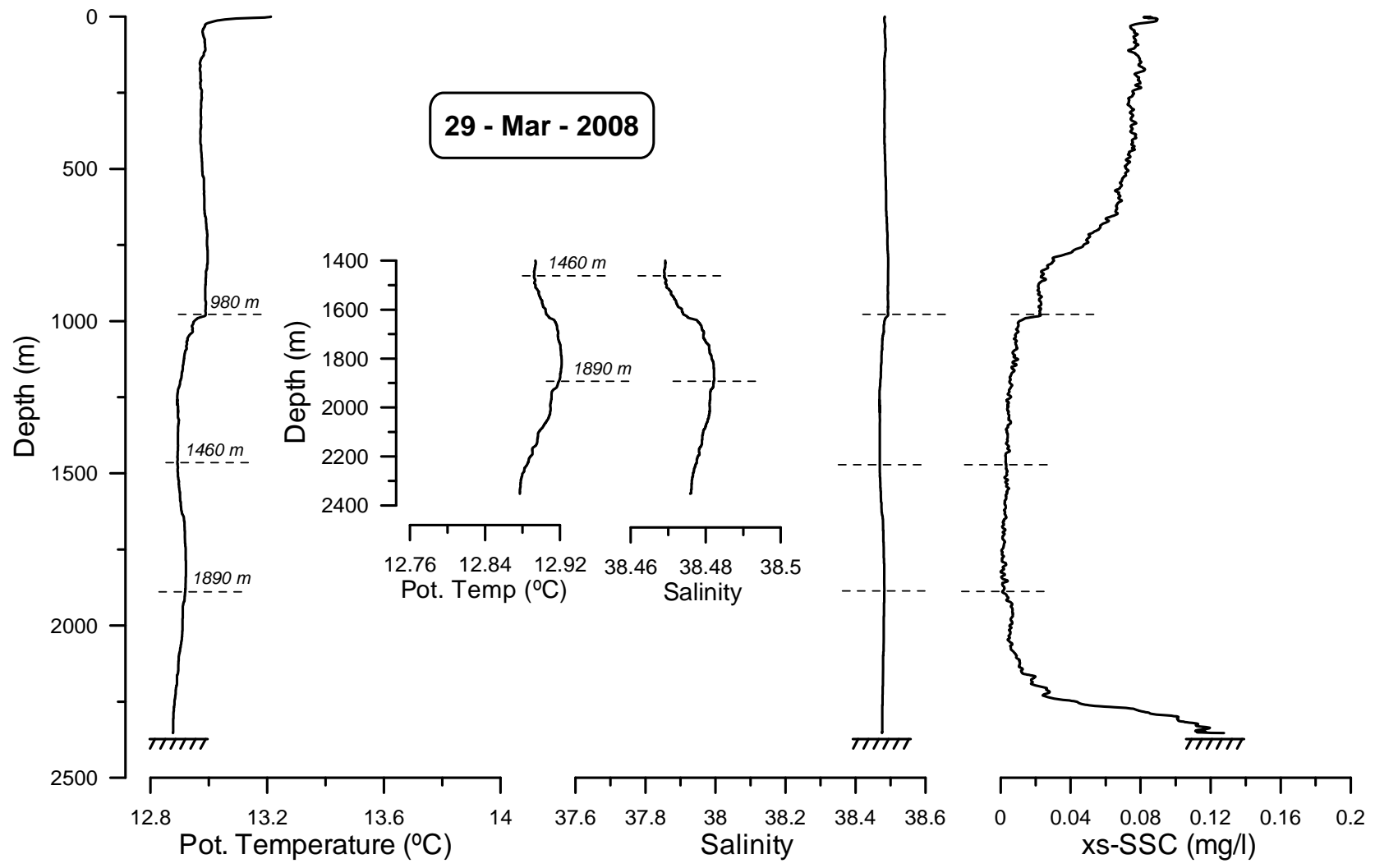
Figure



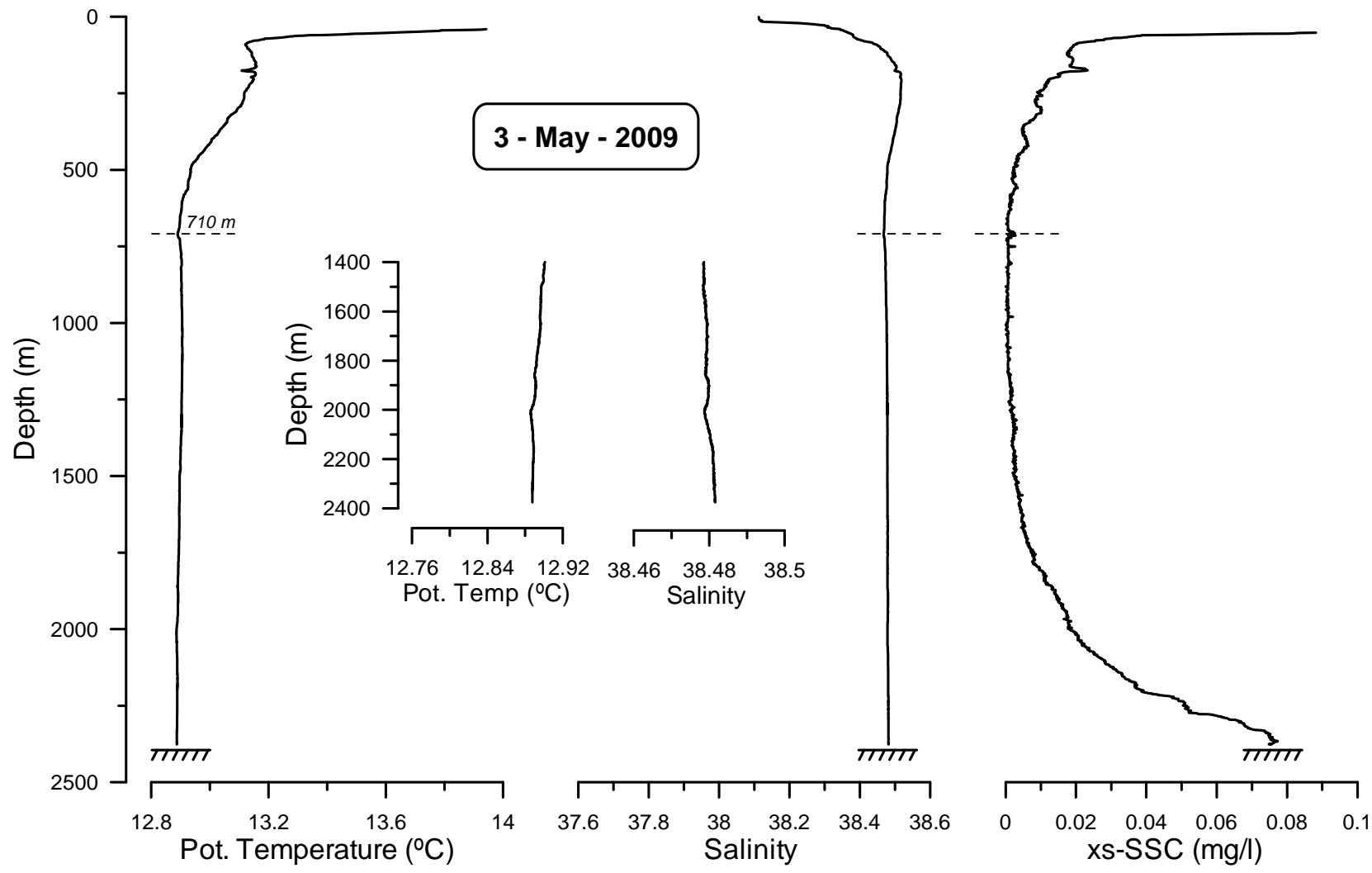
Figure



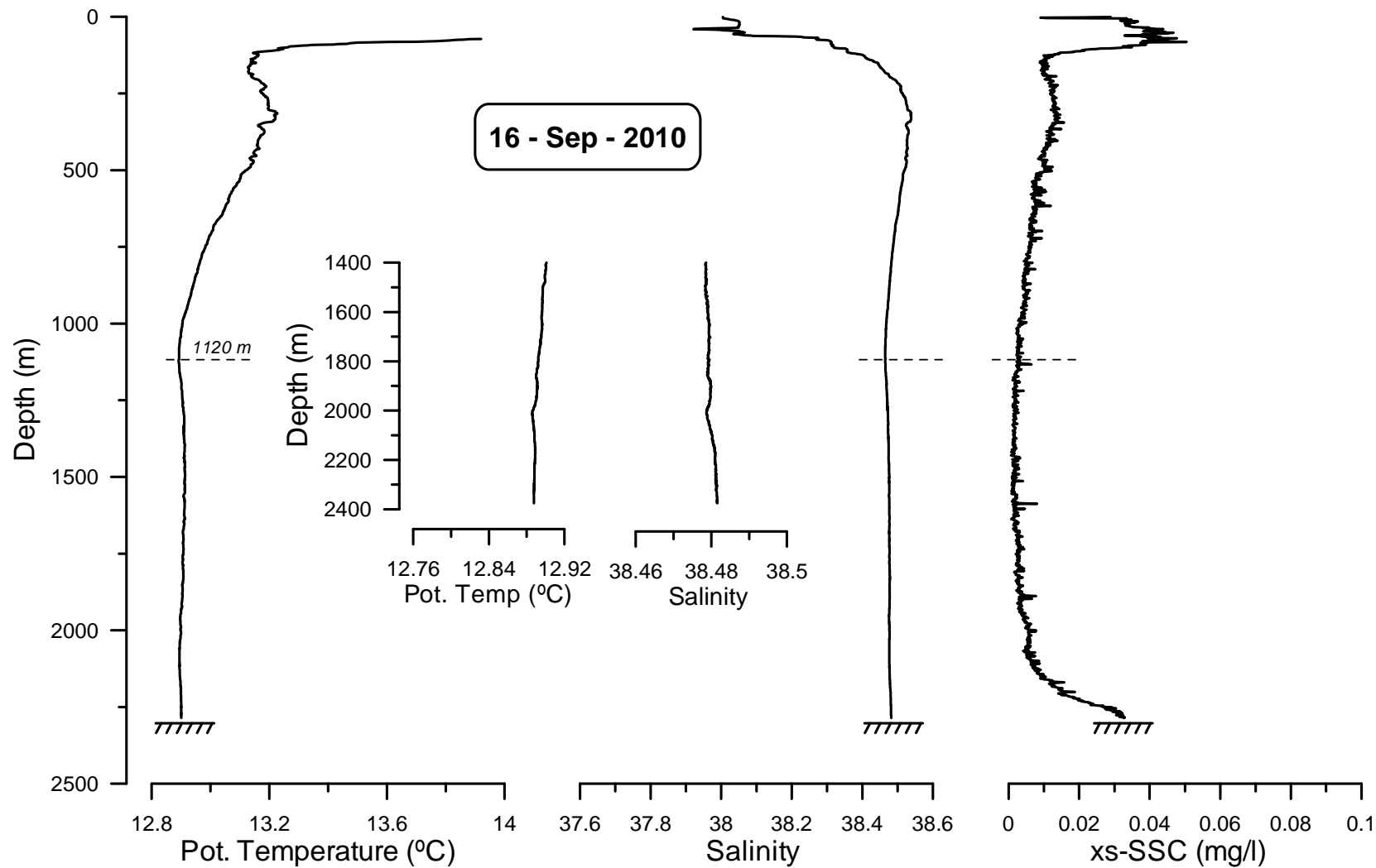
Figure



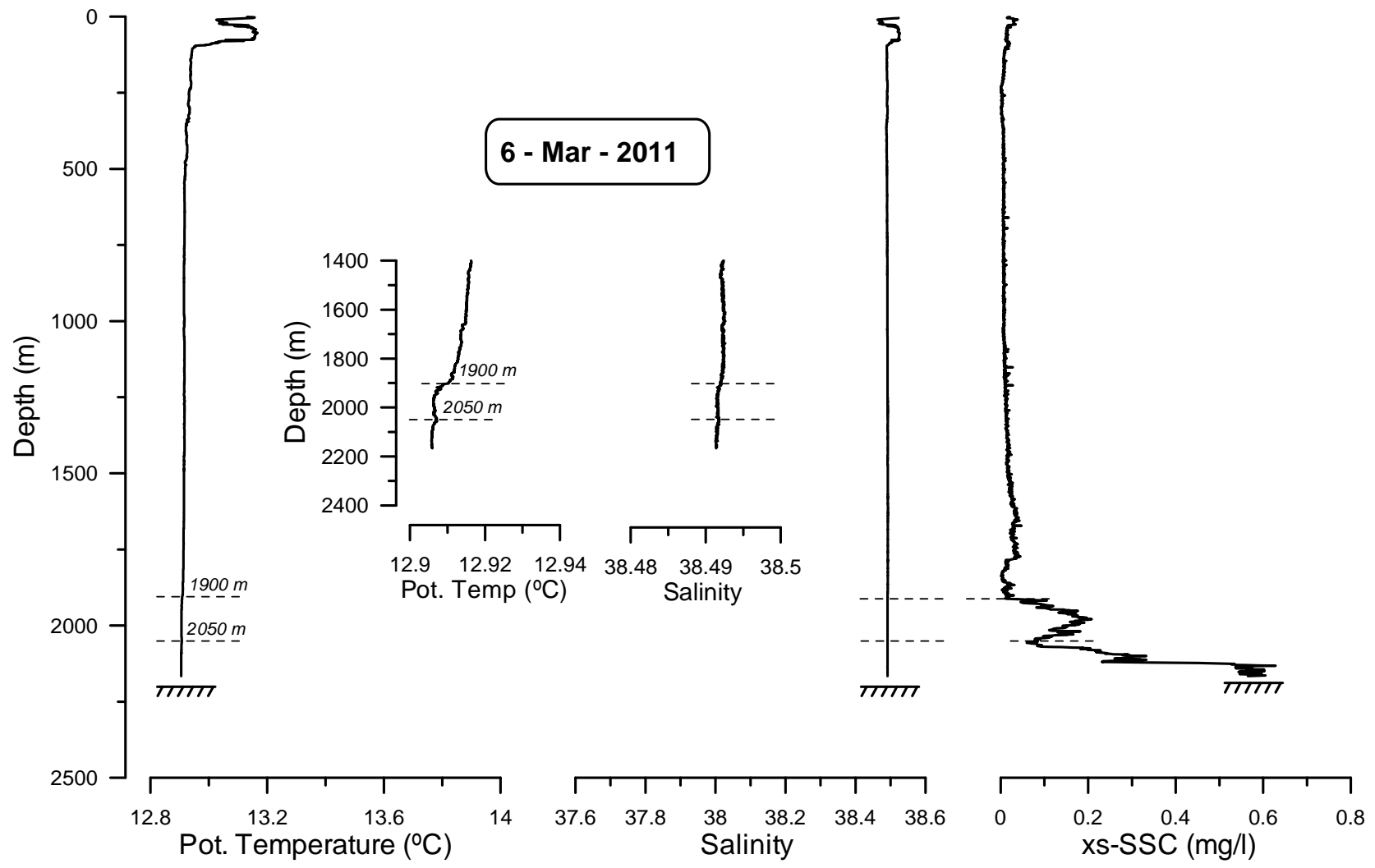
Figure



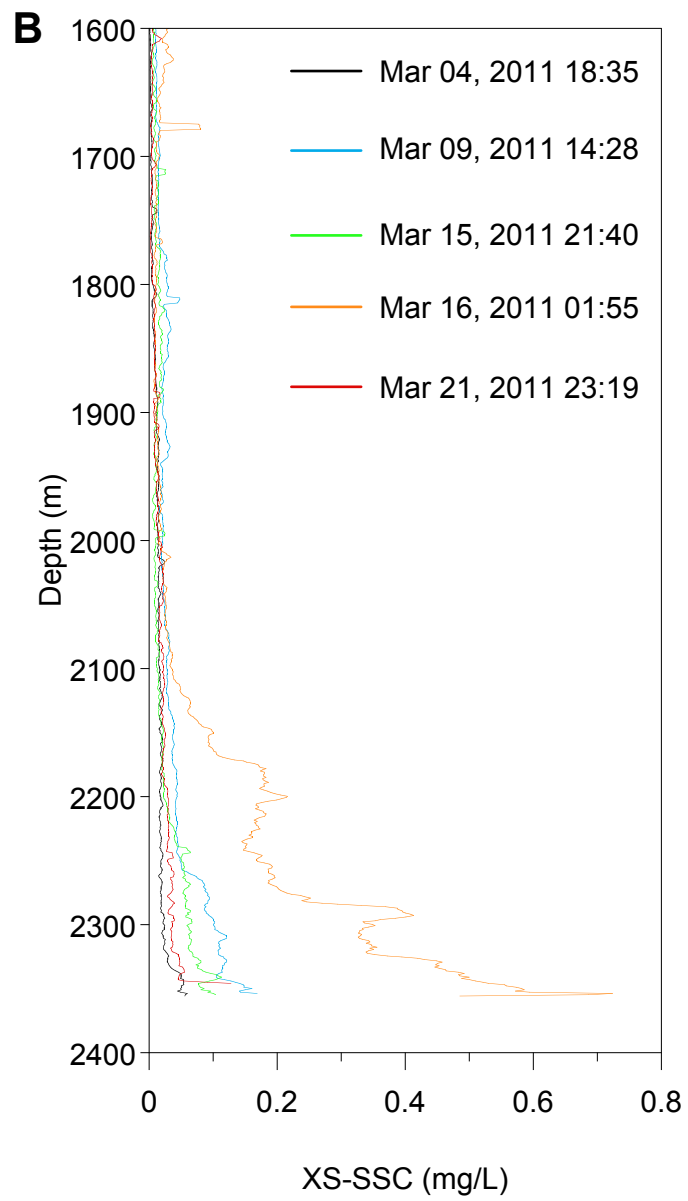
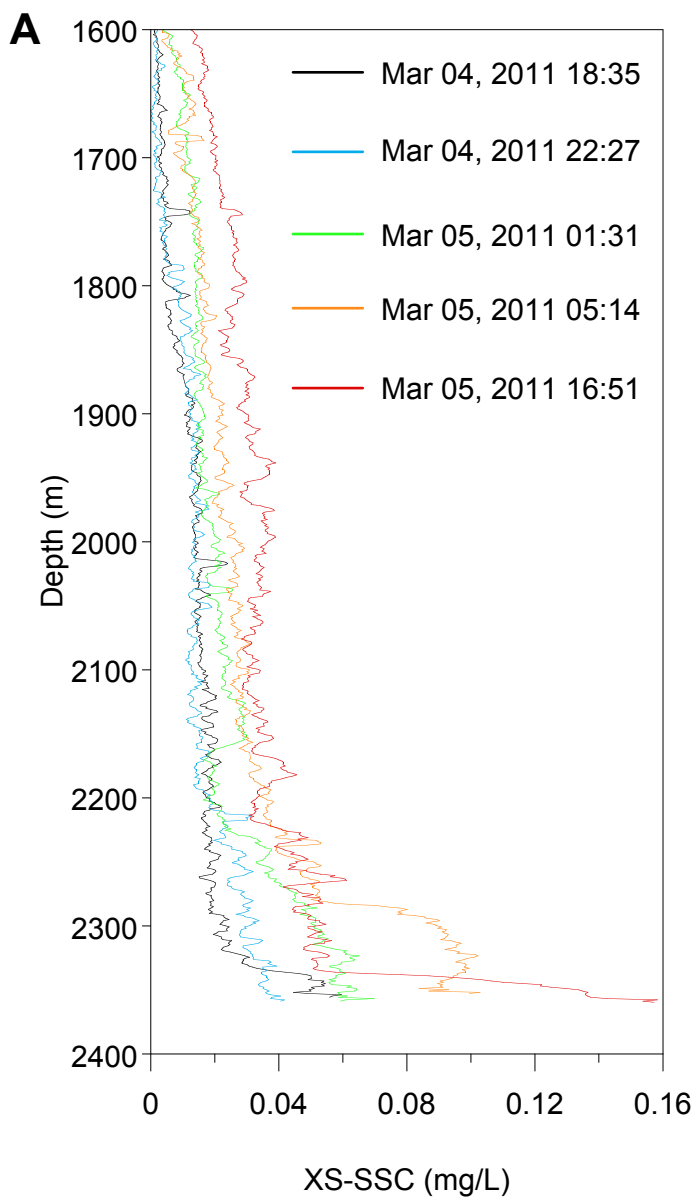
Figure



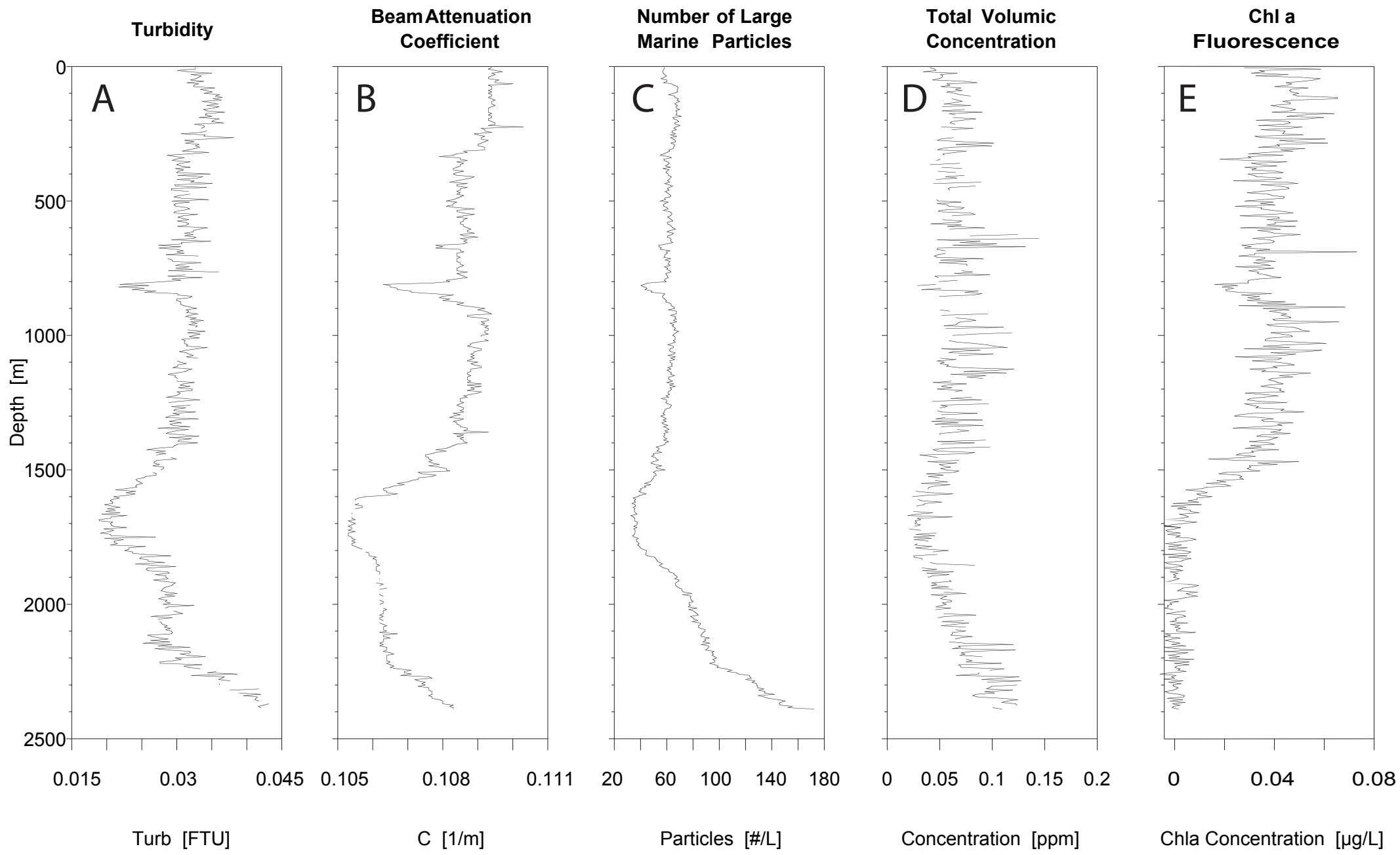
Figure



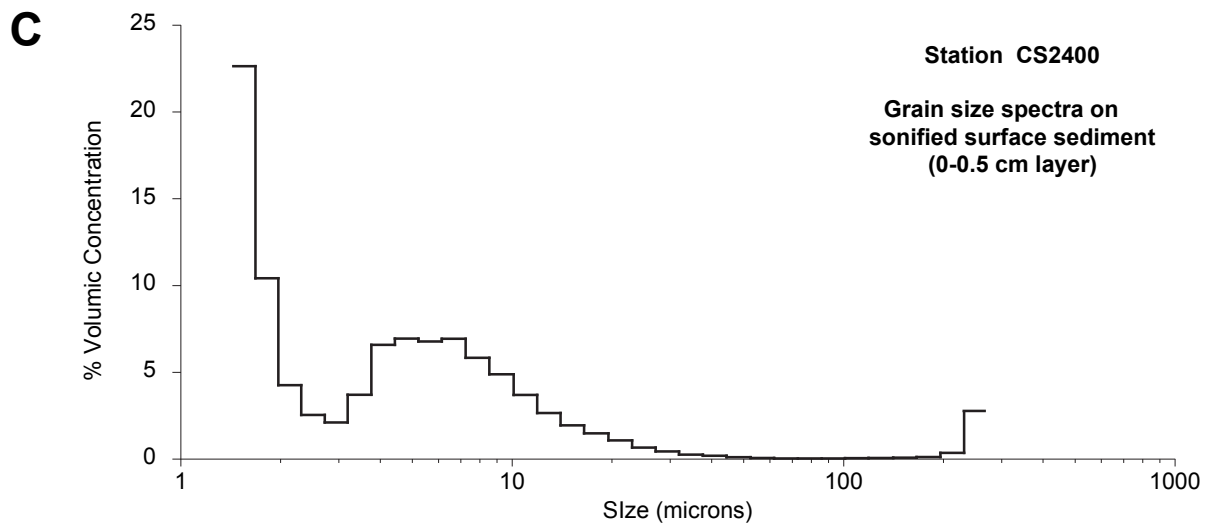
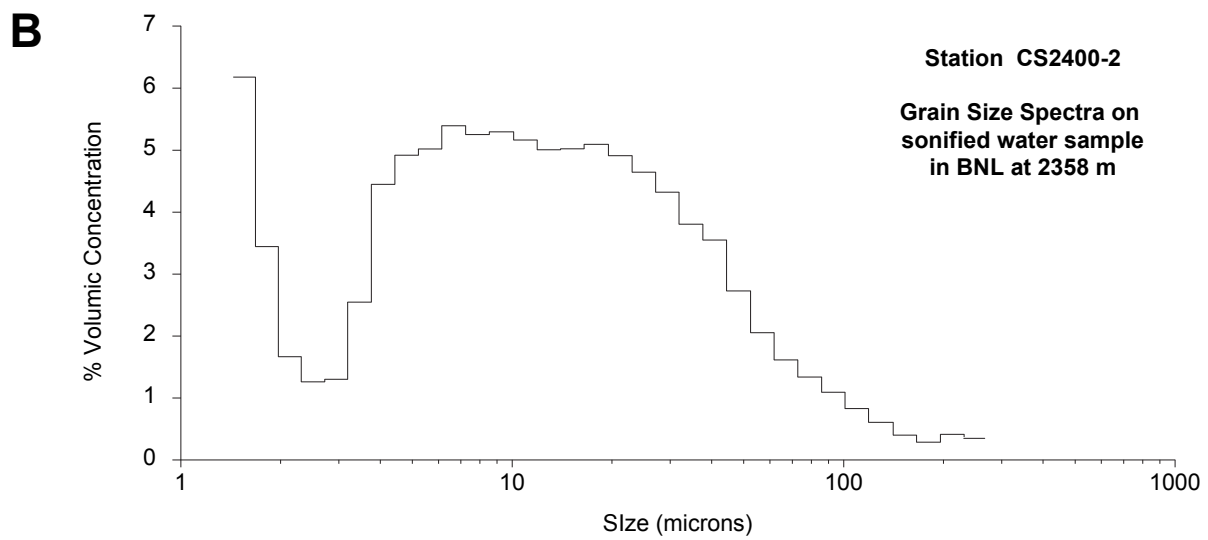
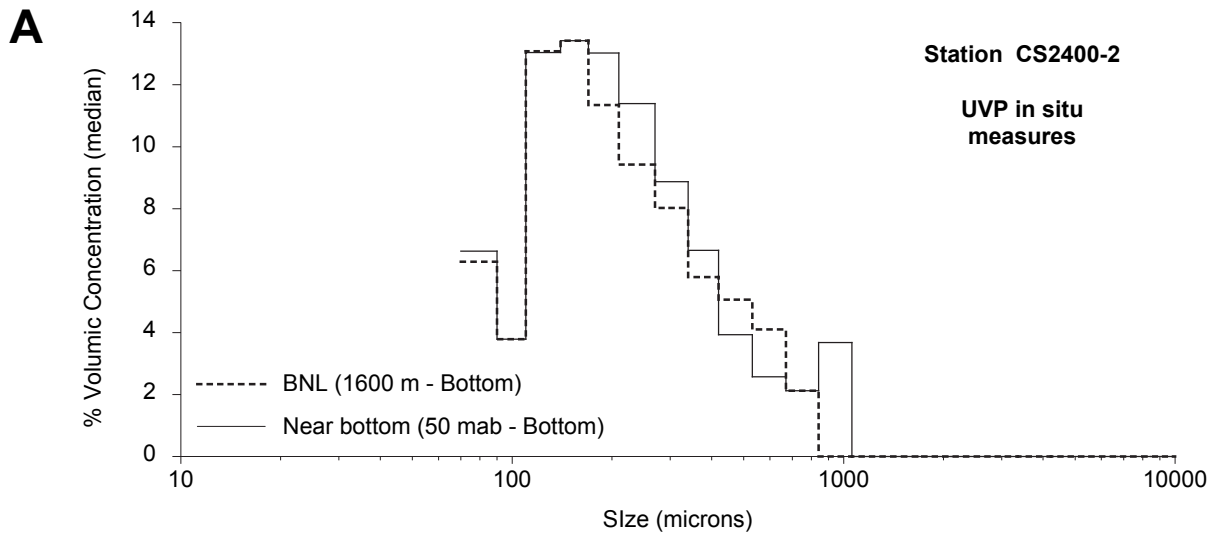
Figure



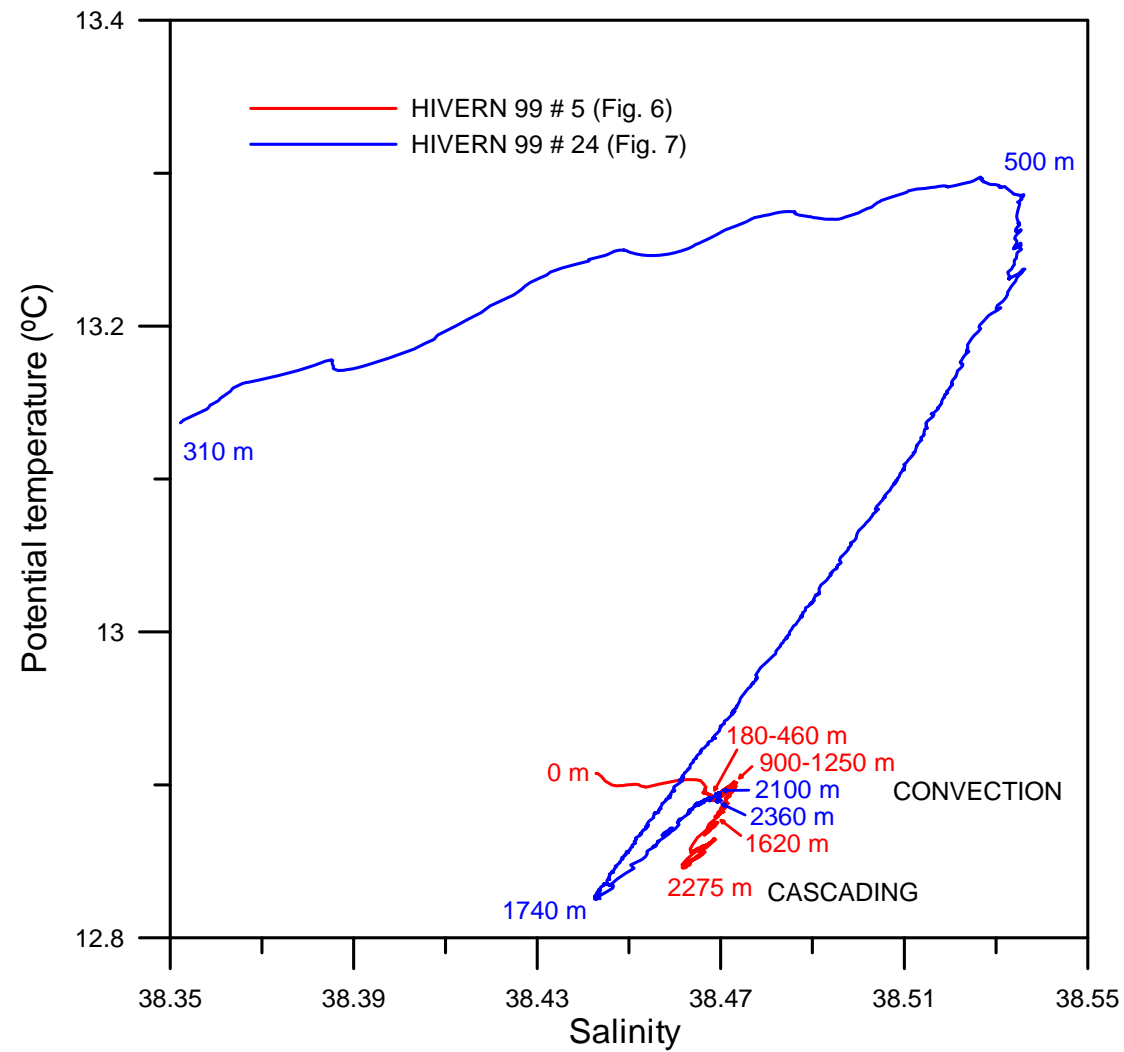
Figure



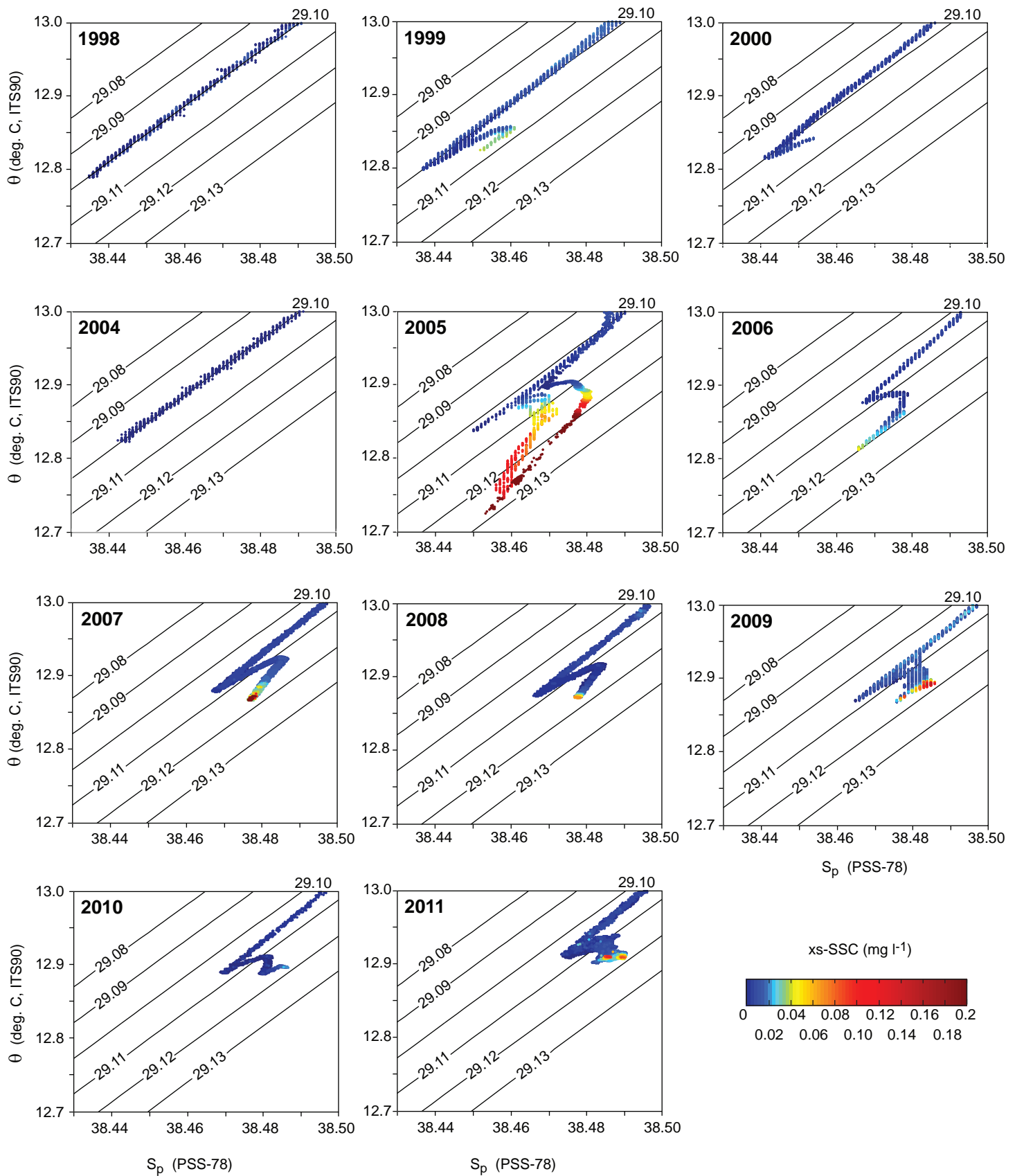




Figure



Figure



Figure

